Nanoindentation Study of the Irrigants Treated Human Premolar

HAIRUL NIZAM BIN RAMLI
(B. Eng. (Hons.), NUS)

A THESIS SUBMITTED
FOR THE DEGREE OF MASTER OF ENGINEERING
DEPARTMENT OF MECHANICAL ENGINEERING
NATIONAL UNIVERSITY OF SINGAPORE

2007

ACKNOWLEDGEMENTS

The author would like to extend his sincere gratitude and appreciation to:

1. Dr Lim Chwee Teck for his valuable guidance and supervision to this project.
2. Dr Anil Kishen and Dr Zeng Kaiyang for their constant support and assistance to this project.
3. Dr Sum Chee Peng for his contributions and guidance to this project.
4. Saji George and Adeela Rafique for helping me in getting fresh samples.
5. Mr Lance Kuhn from Hysitron Inc. for his technical support in using the nanoindentor.
6. Miss Eunice Tan for her help during the course of this project.
7. Fellow laboratory mates for their help, encouragement and friendship.
8. My wife, Norlizah, for her constant support and encouragement.
9. My family and all others who have made this project possible.

TABLE OF CONTENTS

SUMMARY

Root canal treatment is needed to prevent an infected tooth from being extracted. The infected pulp of the tooth is removed and the canal is cleaned and shaped. Ethylenediamine tetraacetic acid (EDTA) and sodium hypochlorite (NaOCl) are the commonly used irrigants in this process. EDTA is used to remove the smear layer in the root canal preparation and kill bacteria. NaOCl is used to dissolve the pulp tissue and destroy bacteria.

In this study, the AFM was used to image the dentin surfaces and the nanoindenter was used to probe the mechanical properties of the teeth. It was found that after sample preparation, smear layers were formed on the dentin surfaces.

The application of 17% EDTA for 5 minutes was effective in removing this smear layer. However the hardness and Young's modulus decreased after the treatment for both the top and bottom surfaces of the dentin sample. The main reason was due to the demineralization of dentin caused by EDTA. Also, surface alterations might further influence the change in the mechanical properties.

When 5.25% NaOCl was applied on the dentin surfaces for 1 hour, it was found that the smear layers were also removed. The hardness and Young's modulus were found to be significantly decreased for both the top and bottom surfaces. The main reason was due to the deproteination of dentin caused by NaOCl. Surface alterations could

also change its mechanical properties. The bottom surface which was closer to the pulp was also more affected than the top surface due to the increase in diameter of the tubules and tubules density. Finally, the reduction of mechanical properties of dentin was found to be only dependent on the distance from the pulp and not the planes of the tooth.

LIST OF FIGURES

LIST OF TABLES

LIST OF SYMBOLS

h	penetration depth, μm	22
h_f	final depth of residual impression, μm	22
$h_{\max}$	maximum penetration depth, μm	22
W	applied load, μm	22
$W_{\max}$	maximum applied load, mN	22
S	contact stiffness	22
h_c	contact depth, μm	23
h_s	displacement of the surface at the perimeter of the contact, μm	23
A	contact area, μm^2	23
H	hardness, GPa	23
E	elastic modulus, GPa	24
C	constant in Area function calculations	78
E_r	reduced modulus, GPa	80
m	power law exponent	80
α	geometric constant	80
β	constant for geometric punch	80
E_s	reduced modulus, GPa	81
υ_s	Poisson ratio for sample	81
υ_i	Poisson ratio for indenter	81

CHAPTER 1 INTRODUCTION

1.1 Background

1.1.1 Root canal treatment

Root canal treatment is necessary to remove infected nerves and blood vessels from the pulp chamber and root canals of the tooth. Professionally, it is called an endodontic treatment.

There is a variety of reasons for the infection or inflammation of the nerves. Deep decay, repeated dental procedures on a tooth, a crack or chip in the tooth are all possible causes. Even though there are no visible chips or cracks, a fracture or injury to a tooth may also cause pulp damage.

As a result, many people with root canal problems feel pain and a prolonged sensitivity to heat or cold. Other signs include tenderness to touch and chewing and discoloration of the tooth. There will also be swelling, drainage and tenderness in the lymph nodes as well as nearby bones and gingival tissues [1]. However, at times, there may be no symptoms.

Root canal treatment can save the tooth from extraction. Endodontists will remove the inflamed or infected pulp, clean and shape the canal and fill and seal the space. A

more detailed procedure for the root canal treatment will be described later. About 95% of root canals are successful and the pain does not return [2].

Two main chemicals used in the root canal treatment are ethylenediamine tetraacetic acid (EDTA) and sodium hypochlorite (NaOCl). EDTA is used to remove smear layer in the root canal preparation. NaOCl is a commonly used irrigant when performing endodontics. Thus, the effects of these agents on the mechanical properties of the tooth should be studied.

1.1.2 Atomic force microscopy

The atomic force microscope (AFM) is a widely used imaging tool because of its ability to give high resolution images in both air and liquid conditions. It is not surprising that many studies involving the imaging of various surfaces of the tooth structures such as dentin [3-5], enamel [6-9] and the dentin-enamel junction (DEJ) [10, 11] use the AFM. Thus in this study, the AFM is used for imaging all the samples.

1.1.3 Nanoindentation

Nanoindentation is a relatively new technique that allows mechanical properties such as Young's modulus and hardness of a material to be determined at the sub-micron scale. In the earlier stages, it has been used to study the mechanical properties of thin films and small micro-structural materials [12]. Although nanoindentations indent a very small depth (<1μm), the mechanical properties obtained are assumed to be

representative of the bulk material if it is homogeneous in nature. In recent years, there is an increasing trend of using the nanoindentation technique to study the properties of biological tissues such as bone [13, 14] and teeth [6, 10, 15-18].

1.2 Objectives

The objectives of this project are to:

1) Evaluate the effects of EDTA on the mechanical properties of dentin, and
2) Evaluate the effects of NaOCl on the mechanical properties of dentin.

1.3 Scope

In order to fulfill these objectives, a number of things needed to be achieved. Sample preparation was needed to be done properly and this was achieved with the guidance and assistance of the staffs from the Faculty of Dentistry, National University of Singapore. Proper storage and handling of samples were also crucial prior to and during all stages of the tests. All imaging of the specimens were done using an atomic force microscope (AFM). The nanoindenter was used to find the mechanical properties, namely the Young's modulus and hardness of the samples, before and after treatments. A statistical software, Minitab 14.2, was then used to compare the baseline results with the results of the mechanical properties after treatment.

1.4 Organization of thesis

In this thesis, chapter 2 starts with a brief introduction of the structure of teeth. However, the main focus is on dentin, and hence, its physical and chemical properties are discussed in greater detail. Then, some literature studies on the root canal treatment are presented. The working principles behind the AFM and nanoindenter and their applications are then discussed. Chapter 3 describes the experimental procedures, namely the sample preparation and the testing method. Chapter 4 presents all the experimental results as well as the statistical results obtained from the experiments followed by the discussions on the effects of EDTA and NaOCl. Chapter 5 provides the conclusion to this thesis and some recommendations in terms of future work is found in chapter 6. The thesis ends with appendices showing the derivations behind the theory on nanoindentation, the individual indentation data, various calculations and the statistical analysis using the Minitab 14.2.

CHAPTER 2 LITERATURE REVIEW

2.1 Tooth Structure

Humans have two sets of teeth, the baby teeth (or known as the primary teeth) and the permanent teeth (also known as the secondary teeth). Initially, children will have 20 primary teeth. However, as they grow older, the primary teeth are replaced by 32 permanent teeth. This section briefly describes the morphology of tooth. Figure 2-1 shows an anatomy of a human tooth.

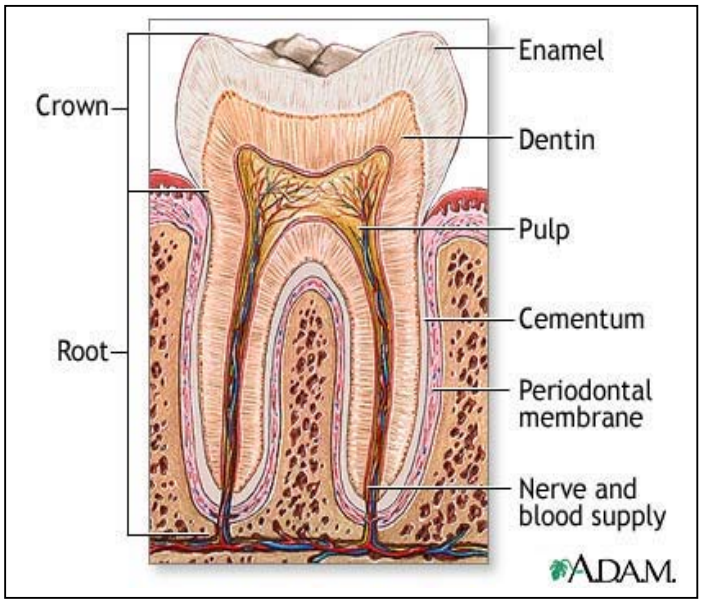

Figure 2-1: Anatomy of tooth [19]

The part of the tooth that is visible in the mouth is called the crown. The size of the crown varies considerably according to age and also the conditions present in the mouth of each person.

The root of the tooth is the portion that is not visible in the mouth. The number of roots can range from one to three. The portion of the tooth that is covered by the cementum is known as the anatomical root.

The enamel is the tough, shiny and usually white outer surface of the tooth. Enamel is semi-translucent and the crown of healthy teeth appears yellowish-white [20]. This is the colour of enamel that is being modified by the underlying dentin. The enamel on deciduous teeth appears much whiter as it is more opaque than the non-deciduous enamel. Enamel is the hardest tissue in the body [21]. Therefore, this property enables enamel to limit the amount of wear and is able to withstand heavy loads of mastication. Enamel has a low tensile strength and is considered to be brittle. However, it has a high modulus of elasticity and the possibility of fracture is minimized due to the flexible support of the underlying dentin.

The dentin is the hard but porous tissue that is under the enamel and cementum of the tooth. Dentin is generally harder than bones but softer than enamel. As dentin is an important structure and the region specifically tested in this study, more of its physical properties and chemical composition is described in the next section.

The pulp is the soft tissue found in the centre of the tooth. It contains blood vessels and nerves and provides nourishment to the dentin. Once infected or inflamed, root canal treatment might be performed to save the tooth. When this tissue is removed, the occupying space is called the pulp cavity.

The cementum is a layer of tough, yellowish, bone-like tissue that is covering the root of the tooth. One of the main functions of the cementum is to help hold the tooth in the socket.

The periodontal membrane is the fleshy like tissue that is between the tooth and its socket. The membrane contains fibers that are embedded within the cementum.

2.2 Dentin

2.2.1 Physical properties

The colour of dentin is pale yellow. It gives the crown its colour since the enamel is semi-translucent. It is generally harder than bone and cementum but is softer and less brittle than enamel. Dentin also has greater compressive and tensile strength compared to enamel. The dentin is made up of intertubular dentin with tubules that are surrounded by peritubular dentin. Figure 2-2 shows an AFM image of dentin.

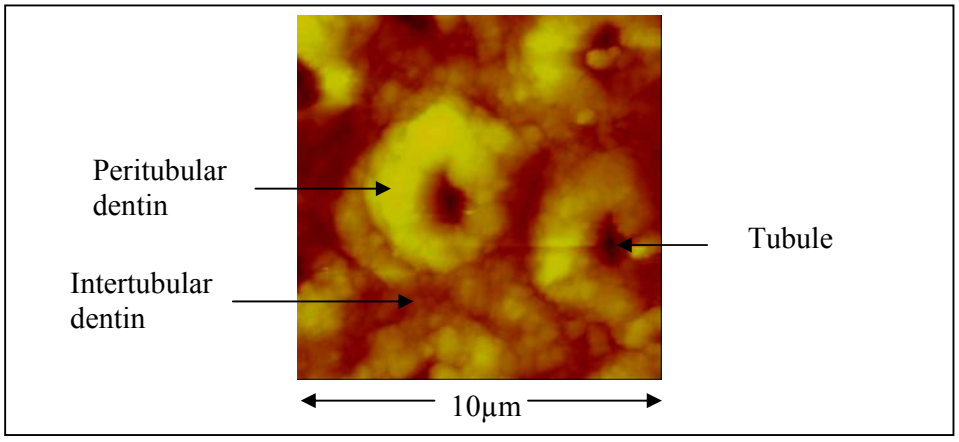

Figure 2-2: An AFM image of dentin

Kinney et al [17] found that the peritubular dentin is much harder than the intertubular dentin. Peritubular dentin is also known as peritubules. Due to the small size of the peritubules, all indentations done in this study are on the intertubular dentin.

Dentin is readily permeable due to the presence of tubules. There are also differences in permeability which are reflected by the regional variations in the tubule size and density.

2.2.2 Chemical composition

The composition of dentin is approximately 70% inorganic material, 20% organic material and 10% water by weight. The same components comprise 47%, 32% and 21% by volume, respectively. The non-mineral component is much higher than in enamel. The main inorganic component in dentin is hydroxyapatite while the main organic component is Type I collagen.

2.3 Root canal treatment

Root canal treatment is performed to save an infected tooth from being extracted. Endodontists use root canal treatment to find the cause and treat problems of the tooth's soft core or dental pulp. When the pulp is diseased or injured and cannot repair itself, it will die. The most common cause of pulp death is either a cracked tooth or a deep cavity. When either of these problems happens, germs or bacteria will enter the pulp and cause infection of the tooth. If left without any treatment,

pus will form at the tip of the root, in the jaw bone, forming a “pus-pocket” called an abscess. Figure 2-3 shows an example of abscess at the root tip.

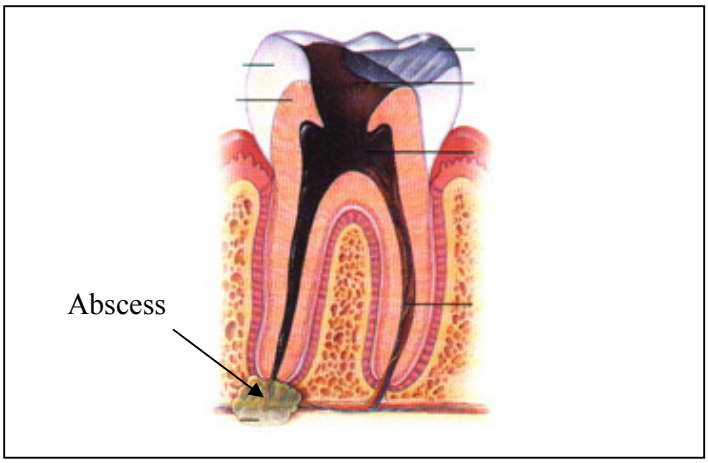

Figure 2-3: Abscess at the root tip [22]

An abscess can also cause serious damage to the bone around the teeth. If the infected pulp is not removed, pain and swelling will occur. Without any treatment, the tooth may have to be removed. To prevent this, a root canal treatment is performed. Figure 2-4 shows the procedure of the root canal treatment [22].

	Procedure
	Step 1: Anesthesia is given to the patient. An opening is made into the pulp of the tooth.
	Step 2: To determine the length of the roots, files are place into the canal.
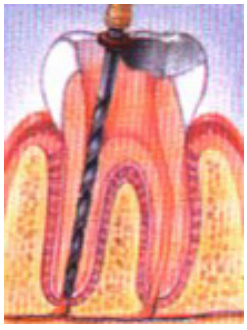	Step 3: The canals are then cleaned and shaped by using threadlike rotary instruments. Together with irrigation, the infected pulp tissue is removed.
	Step 4: A biologically compatible material called *gutta percha* is used to seal the root canals.

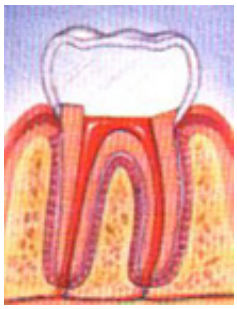	Step 5: A crown or other restoration is placed on the tooth to protect it and restore to full function.

Figure 2-4: Root canal treatment procedures [22]

If the tooth lacks sufficient structure to hold the restoration in place, a post may be needed to be placed inside the tooth.

In Step 3 of Figure 2-4, irrigation is also used to remove the infected pulp. Copious amounts of irrigating solution should be used in cleaning and shaping of the root canal [23]. This serves to flush out debris, eliminate microorganisms and lubricate the root canal instruments. The irrigating solution used should have disinfecting and pulp tissue-dissolving properties. EDTA and NaOCl are the common irrigants used in the root canal treatment.

EDTA is an irrigant commonly used by dentists to remove the smear layer at the end of the root canal preparation. The common concentrations used are 15-17% di-sodium EDTA [24]. O'Connell at el [25] reported that EDTA is usually applied at a 17% concentration. Therefore, in this study, we used 17% EDTA at pH 7.2.

Although smear layer removal remains controversial, there can be many benefits in removing this layer or organo-mineral [26]. Removal of the smear layer not only improves the seal of the root fillings, it also removes bacteria, toxins and remnant pulpal tissues that may be present in the smear layer [27].

Past studies used different durations to apply EDTA to dentin [24, 28, 29]. Calt and Serper [28] studied the time-dependent effects of EDTA on dentin by irrigating dentin for 1 to 10 minutes while Nygaard-Ostby [29] applied EDTA for 5 minutes. In this study, we will also apply EDTA to dentin for 5 minutes and get the images and mechanical properties. If possible, we will continue applying EDTA for another 5 minutes to see if there are any changes.

NaOCl is also used commonly as an irrigant when performing endodontics and is taught in many schools in North America and Europe [30]. NaOCl irrigation is also widely practiced in Australia, Asia and other countries [27]. NaOCl is used in endodontics for two main purposes, which is to dissolve pulp tissue and to destroy bacteria [31, 32]. It is a very reactive and toxic compound.

In endodontics, concentrations of 0.5% to 5.25% NaOCl are regularly used [27]. Although NaOCl is the most commonly employed root canal irrigant to date, there are no existing general agreement regarding its optimal concentration, which is 0.5% to 5.25% [33]. It is observed that specialists were more likely to select a higher concentration than general practioners practicing endodontics, as

specialists might want a more thorough therapeutic effect or a shorter treatment time [27].

Berber et al [33] tested the efficacy of various concentrations of NaOCl with various instrumentation techniques to reduce the bacteria within root canals and dentinal tubules. The result suggested that 5.25% NaOCl has a greater antibacterial activity inside the dentinal tubules than the other concentrations used. Therefore in this study, we used 5.25% NaOCl with pH 11.

2.4 Atomic Force Microscopy

The AFM is probably the most versatile member of a family of microscopes known as the scanning probe microscopes (SPMs). Scanning probe microscopy began in the early 1980s when Binnig, Rohrer, Gerber and Weibel at IBM in Zurich, Switzerland, revolutionized microscopy through the invention of scanning tunneling microscope (STM) in 1982. The importance of this discovery was recognized through the Nobel Prize in Physics which was won by Binnig and Rohrer for this invention in 1986.

Also, in 1986, as a collaboration between IBM and Stanford University, Binnig, Quate and Gerber developed the AFM [34]. The emphasis initially was mainly to improve the imaging resolution compared to the optical microscope and also to overcome the limitations of STMs, which was the inability to image non-conducting samples.

The AFM has since then evolved into a useful tool not only for its atomic resolution topographic imaging capabilities, but also for its direct measurements of intermolecular forces with atomic resolution characterization. This can be employed in a broad spectrum of application such as electronics, semi-conductors, materials, manufacturing, polymers, biology and biomaterials.

Also, the ability to give high resolution images in both air and liquid conditions, gives the AFM an advantage over certain other microscopes. In this study, the AFM is used for all imaging purposes.

2.4.1 Working principle of AFM

A typical AFM system consists of a micro-machined cantilever probe and sharp tip that is mounted on a piezoelectric actuator and a position sensitive photo detector. The AFM cum nanoindentation system used in this study comprises the Nanoscope IIIa controller (Digital Instruments, Santa Barbara, CA, USA) with the standard head interchangeable with a Triboscope indenter system (Hysitron Inc., Minneapolis, MN, USA) as previously described [35]. Figure 2-5 shows the AFM used.

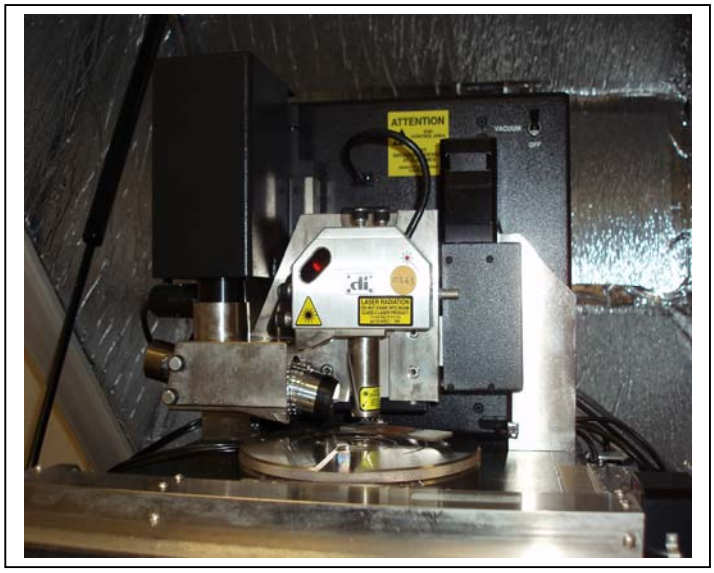

Figure 2-5: An AFM set-up

A sharp tip at the free end of the cantilever is systematically scanned across the surface of the sample to generate a topographical image of the sample. The extension and retraction of a piezo ceramic crystal infers fine position control. As the tip tracks the surface of the sample, the forces between the tip and surface causes the cantilever to bend. Laser light from a solid state diode is reflected off the back of the cantilever and is collected by a position sensitive photo detector. Figure 2-6 shows a schematic drawing of the beam deflection system.

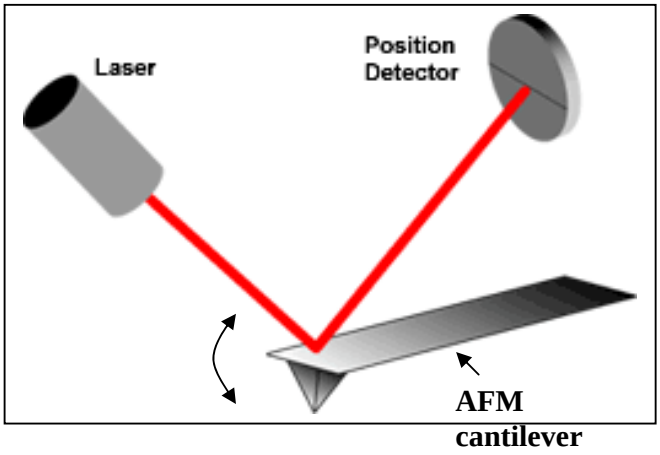

Figure 2-6: Beam deflection system [36]

The detector consists of two closely spaced photodiodes whose output signal is collected by a differential amplifier. The angular displacement of the cantilever will result in one photodiode collecting more light than the other and this will produce and output signal which is proportional to the deflection of the cantilever. The amount of feedback signal, measured at each scanning point of a 2-D matrix, can be collected to form a 3-D reconstruction of the sample topography and usually displayed as an image.

The AFM consists of an XYZ translator, cantilever with tip, deflection sensor and a control unit with image processing.

There are 3 main imaging modes of the AFM. They are the contact mode, non-contact mode and tapping mode. There are different advantages and disadvantages from these 3 modes and hence, different applications uses different imaging mode. In this study, the imaging mode that is used is the tapping mode. The

tapping mode is a hybrid of contact and non-contact modes where a vibrating cantilever is held above the sample surface as it scans. The tip intermittently comes into contact with the surface. The intermittent contact serves to reduce the lateral force incident on the sample, therefore reducing surface damage and tip contamination but still able to maintain high imaging resolution. This mode can be used in both ambient and liquid conditions which makes it suitable for this study. Other considerations for the tapping mode for this study include no lateral scrapping and faster scan speed than contact mode AFM.

2.4.2 Atomic force microscopy of teeth

There are many studies that used AFM to image biological materials like cells [37-41], proteins [42-45] and hard tissues like bones [46-48] and teeth [5-7, 16, 49-55].

Lippert et al [7] investigated the effects of demineralization and remineralization cycles at human tooth enamel surfaces by AFM. He used the tapping mode to image the enamel at various stages of demineralization.

Chng et al [55] used the AFM to compare the effects of 30% hydrogen peroxide on the dentin. The images obtained by the AFM shows distinct differences in surface structure and roughness.

Ho et al [56] also used the AFM to investigate the effect of sample preparation technique on determination of structure and nanomechanical properties of human cementum hard tissue.

These studies are examples to illustrate that AFM is a very powerful tool in studies that require the imaging of teeth. The AFM is able to image almost any part of the teeth with such high resolution that we are able to see if there are any changes in the microstructure or roughness of the surface. As such, the AFM is used in this study.

2.5 Nanoindentation

There is always a need to obtain the mechanical properties of materials with spatial resolution in the nanometer range. Techniques like impact testing and even microindentation are not able to achieve such standard. Thus, this has sparked a surge of interest in the field of nanoindentation. With nanoindentation, we can locate exactly where we need to indent in the nanometer range. This is especially useful if we need to extract the mechanical properties of nanostructured materials or small non-homogeneous materials. Figure 2-7 shows a Hysitron nanoindenter used for this study.

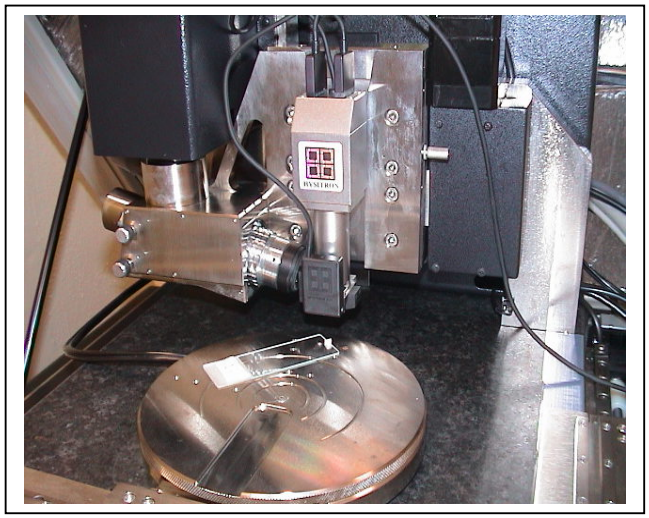

Figure 2-7: A Hysitron nanoindenter

The nanoindenter comprises a load-sensing piezoelectric transducer, a displacement sensing unit, a x-y translator stage and an indenter tip. Figure 2-8 shows the schematic diagram of a nanoindentation system.

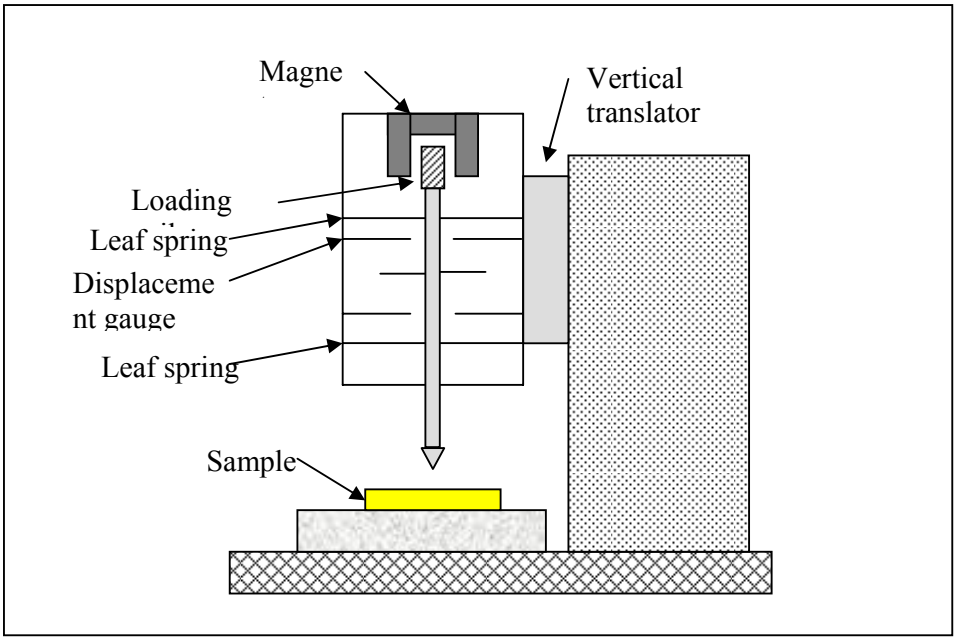

Figure 2-8: Schematic diagram of a nanoindenter

There are a lot of tips that can be used for indentations. The geometry of the tip can be blunt or sharp. The spherical tip is an example of a blunt indenter while sharp indenters include the Berkovich, Knoop and Vickers tips. The use of these tips varies with applications. However, the diamond Berkovich tip is most commonly used to scan and indent samples. Figure 2-9 shows a Berkovich tip that is similarly used in this study.

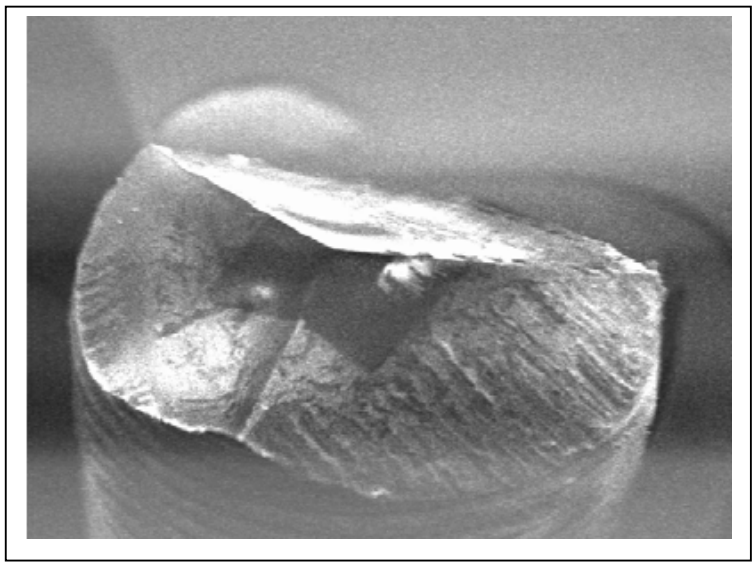

Figure 2-9: A Berkovich tip [57]

Although the Berkovich tip can be used to scan the topography of the sample, a nanoindenter is rarely used for imaging purposes solely. The resolution of the images obtained is not as high as the AFM. This is because the tip radius of the Berkovich tip is 10 times more than the AFM tip. Therefore, the images obtained during scanning here are used mainly to locate a suitable and relatively flat position for indentations to be carried out. For higher resolution images, an AFM is usually used.

The earlier nanoindentation systems made use of optical microscope to image the sample before indentation. Recently, most nanoindentation systems incorporate an AFM module.

Due to the high resolution of displacement and small force involved in nanoindentation tests, it is crucial that inaccuracies arising from environmental factors such as temperature changes, noise and vibrations are minimized [58]. Placing the equipment on a vibration isolation table as well as housing the equipment in an environmental isolation enclosure helps. Certain softwares are also able to provide corrections to compensate for the thermal drift.

Sample preparation is also very important. For proper preparation, the roughness of the surface that will be indented on must be less than one-tenth of the maximum indent depth. Therefore, a relatively smooth site is needed for indentation. Furthermore if the sample is placed on a substrate, the indentation must not be more than one-tenth of the height of the sample. Otherwise, the mechanical properties of the supporting substrate might come into effect and the readings will not be accurate.

Also, most nanoindenters are able to conduct tests on the sample in both and wet conditions. This is particularly useful especially for samples that need constant hydration like teeth.

2.5.1 Working principle of nanoindenter

During indentation, a curve describing the relationship between the load W and the displacement h is continuously monitored and recorded. Using the method described by Oliver and Pharr [59], the mechanical properties of the material can be derived through the analysis of the load-displacement data during the loading-unloading indentation cycle. At peak load, the load and the displacement are W_{max} and h_{max}, respectively. Figure 2-10 shows a schematic representation of the loading-unloading curve and some of the quantities that are used in the calculation of hardness and Young's modulus. Figure 2-11 shows a schematic representation of a section through an indentation.

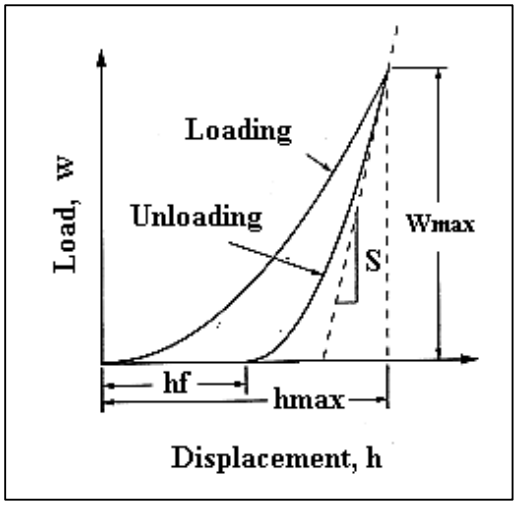

Figure 2-10: Load-displacement curve for an indentation experiment

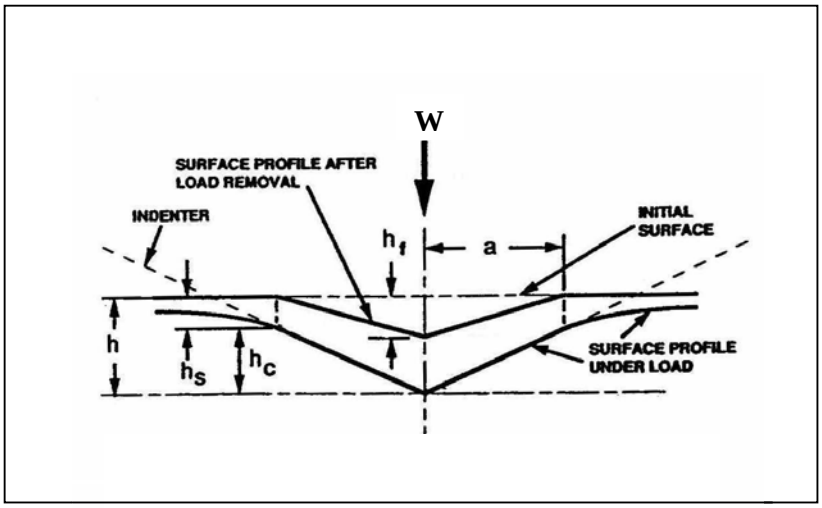

Figure 2-11: Schematic representation of a section through an indentation

The total indentation depth measured, h, is the summation of h_s, which is the displacement due to elastic deformation and h_c, which is the contact depth or the depth of the indenter in contact with the sample under load. The final depth, h_f is the depth when the indenter is fully withdrawn.

2.5.1.1 Hardness

The hardness is derived from the applied load divided by the projected area of the indentation. Using the method described by Oliver and Pharr [59] earlier, the hardness is given by the equation (2.1),

$$H = \frac{W_{\max}}{A} \qquad (2.1)$$

where W_{max} is the maximum applied load and A is the area function. The hardness can be change accordingly to the area function input. Therefore, the tip must be frequently calibrated against the standard fused quartz for more accurate results. Appendix A shows a detailed derivation of the hardness.

2.5.1.2 Young's modulus

The Young's modulus is derived by using the initial slope of the unloading curve (dW/dh) where it is assumed to be the elastic displacement of the specimen. Similarly, using the method of Oliver and Pharr [59], the Young's modulus of the sample, E , is given by the equation (2.2),

$$E = \frac{\sqrt{\pi}}{2\sqrt{A}} \frac{dW}{dh} \qquad (2.2)$$

where dW/dh is the slope of the unloading curve at maximum load or also known as the stiffness, S. A detailed derivation of the Young's modulus is shown in Appendix B.

2.5.2 Nanoindentation of teeth

Nanoindentation technique has been widely applied for metals. However, there is an increasing use of the technique to determine the properties of biological materials like bones [13, 14] and teeth [6, 10, 15-17, 60]. Before nanoindentation testing, researchers had to resort to micro testing. This posed an obvious problem, especially in the determination of dentin hardness and modulus, because the indentations are considerably large. As a result, the microindenter could only provide a composite average and could not separate the effects on dentin properties that are due to morphology and those due to composition. For example, using a microindenter, Pashley et al [61] suggested that the decrease in hardness on approaching the pulp can be attributed to the increase in the number of tubules. However, Kinney et al [17], using the nanoindenter, found that the decrease can be attributed to the changes in hardness of the intertubular dentin itself and not

due to the number of tubules. This proves that the nanoindenter is a very powerful tool in the characterizing the mechanical properties of materials, especially those that have variations on a small scale.

Therefore, the nanoindentation technique is applied to test different parts of the tooth. Some studies attempt to characterize enamel by determining its mechanical properties [6, 7, 15, 16, 18]. Cuy et al [15] used nanoindentation to investigate the mechanical properties of enamel over the axial cross-section of a maxillary second molar. Lippert et al [7] investigated the possible rehardening of surface softened enamel in two separate experiments. Habelitz et al [62] studied the mechanical properties of single enamel rods at different orientations at the cusps area.

Although a lot of studies have used nanoindentation, due to the difficulty in performing these experiments, a wide range of values for hardness and Young's modulus are reported. Habelitz et al [16], for example reported a value of 74 to 80 GPa for Young's modulus and 3.2 to 3.7 GPa for hardness. However, Cuy et al [15]**,** reported values of 66.2 to 91.1 GPa for Young's modulus and 3.4 to 4.6 GPa for hardness.

Similarly, nanoindentation is also the preferred technique for the characterization of nanomechanical properties of dentin. Since dentin consists of the peritubular and intertubular dentin, the indenter tip is small enough to indent on each individual part. Thus both the peritubular dentin and intertubular dentin can be

characterized separately. In the study by Kinney et al [17], the hardness of the peritubular dentin is found to be about 2.45 GPa and its Young's modulus about 29.8 GPa and are independent of location. For intertubular dentin however, the hardness and Young's modulus is lower nearer to the pulp than compared to those nearer to the DEJ. The value for hardness has a range of 0.15 to 0.51 GPa and Young's modulus of 17.7 to 21.1 GPa. Angker et al [63, 64] used nanoindentation to study the mechanical properties of carious dentin. There are also other studies done on dentin using the nanoindentation technique.

Other important studies used this technique as a tool to compare the mechanical properties of dentin before and after exposing them to various agents, drinks as well as storage medium.

Hairul Nizam et al [60] and Chng et al [55] evaluated the effect of 30% hydrogen peroxide, a bleaching agent on the nanomechanical properties of teeth. Popular studies like finding the effects of various drinks also used this technique. Finke et al [6] studied the in situ hardness changes of polished human enamel surfaces after the exposure to three different drinks. Mahoney et al [65] also did a similar study to determine the change in hardness and modulus of elasticity of both enamel and dentin in primary teeth after exposure to potentially erosive beverages.

A very useful study is done by Habelitz et al [16] to find the effects of storage medium on the mechanical properties of enamel and dentin. The samples are

placed in three storage mediums which are deionized water, calcium chloride buffered solution and Hank's balanced salt solution (HBSS). The nanoindentation study showed that storing teeth in deionized water or calcium chloride solution resulted in a large decrease in elastic modulus and hardness. After 1 day, there was a decrease in the mechanical properties values of up to 20% and 30% for enamel and dentin, respectively. After 1 week, the mechanical properties dropped to below 50% of their starting values. The main reason for the drop was due to the demineralization process during storage. However, storing the teeth in HBSS did not significantly alter the mechanical properties for a time interval of 2 weeks and hence it is recommended that the teeth are stored in HBSS. Figure 2-12 shows the changes in the mechanical properties over time in their respective storage medium.

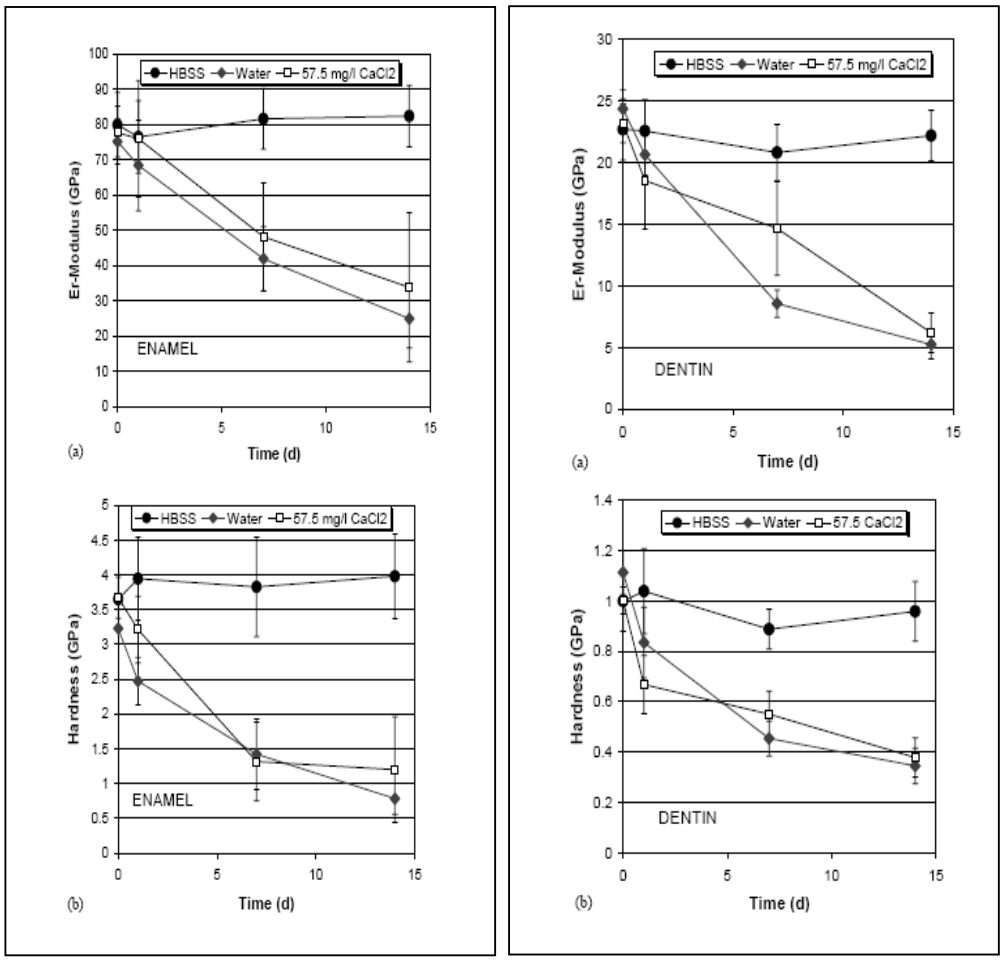

Figure 2-12: Variation of elastic modulus and hardness values over time in enamel and dentin when exposed to deionized water, calcium chloride buffered solution and HBSS [16].

Following this important study, all the teeth used in this experiment were stored in HBSS when not subjected to any test. This was to make sure that any changes in the mechanical properties detected would be due solely to the effects of the agents rather than the storage medium.

Besides enamel and dentin, there were also studies done using the nanoindentation technique on the DEJ. Urabe et al [66] used nanoindentation test to determine the hardness and Young's modulus from the deep enamel to the superficial dentin of human teeth. Similarly, Marshall et al [10] sought to characterize the nanomechanical properties of the DEJ using the same technique. Figure 2-13 shows the hardness and elastic modulus determined from the indentations at location shown on the AFM scan of the DEJ.

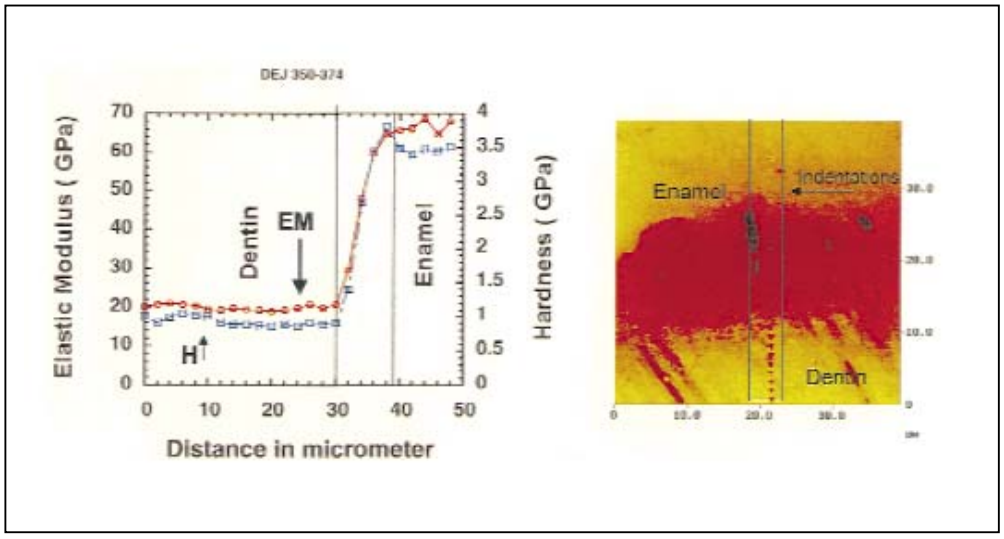

Figure 2-13: Elastic modulus (GPa) and hardness (GPa) against distance (mm) plot and the location of indentations on the AFM scan of the DEJ [10].

From both studies, nanoindentation has been able to demonstrate that the hardness and elastic modulus rose steadily across the DEJ from bulk dentin to enamel.

For all these studies, it is observed that a wide range of values for the mechanical properties of teeth are reported. This is not surprising as different teeth have

different mechanical properties. Variables like age, mouth conditions and certain diseases can affect the mechanical properties of teeth. As we have discussed earlier, even storage medium plays a part. Furthermore, due to the small size of the samples, nanoindentation tests are quite difficult to perform. Preparation and handling are difficult and time consuming. Since there is no standard protocol on the preparation of teeth, different methods of preparation may yield different roughness which can affect the result as well.

In this study the mean values of the mechanical properties before and after treatments with the agents were used to compare the effects on dentin. Therefore the main concern was with the changes in the mechanical properties rather than the absolute values.

It is also known that teeth exhibit creep properties [67, 68]. This information is essential in designing a proper test. In a study by Kinney et al [69], a loading of 400 to 700 μN was applied to the sample. The maximum force was held constant for an unspecified brief period of time before it was decreased linearly back to zero. The holding period was necessary because the presence of creep can dramatically affect the unloading curve. This would cause a 'nose'-like effect to occur as shown in Figure 2-14.

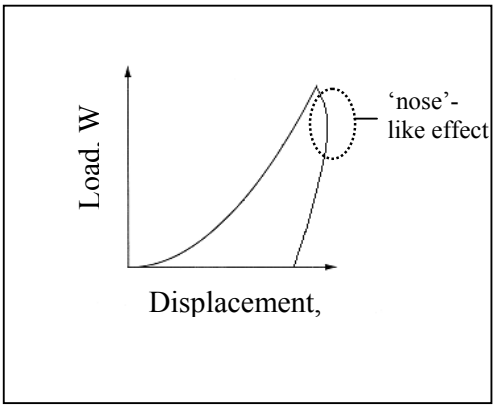

Figure 2-14: 'Nose'-like effect due to creep

As the calculation for Young's modulus involves the gradient of the unloading curve, this will lead to inaccurate values. In extreme cases, the Young's modulus will be negative. From this, it can be concluded that it is necessary to include a holding period at the maximum load, after loading and before unloading, in the test procedures. The load against displacement curve will be similar to the one shown in Figure 2-15 and the correct Young's modulus will be recorded.

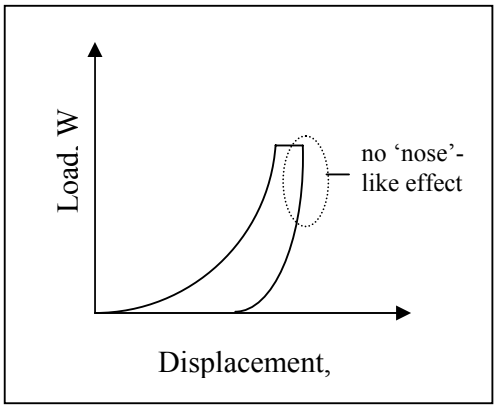

Figure 2-15: Absence of 'nose'-like effect

CHAPTER 3 EXPERIMENTAL DETAILS

3.1 Sample Preparation

3.1.1 Selection of teeth

The dentin samples were harvested from human premolars extracted for orthodontic reasons. The teeth were firstly autoclaved. Then the autoclaved teeth were decoronated and the cementum were carefully scrapped off the surfaces of the root. They were placed in Hank's balanced salt solution until they were ready to be prepared for testing.

3.1.2 Preparation of tooth

Each tooth was then cut with a calcified tissue microtome. This equipment is equipped with a micrometer table that controls the blade traverse and also a mount to hold the tooth. Figure 3-1 shows the microtome used in this study.

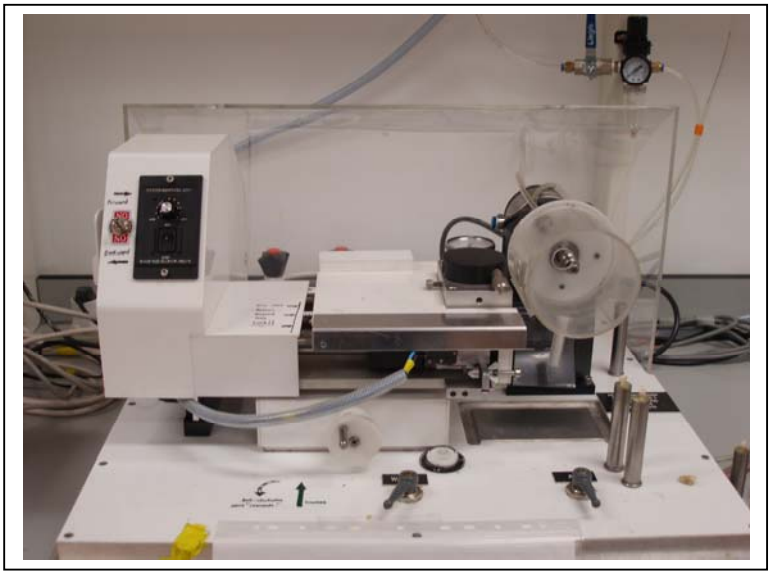

Figure 3-1: Microtome used for sample preparation

The cuts were made using a water cooled diamond blade of dimensions 7.8cm by 0.15mm (Buehler, USA). The root was cut longitudinally, on the mesial, lingual, distal and buccal aspects of the root canal. The first 150 micron of dentin of the root canal wall was eliminated and then another cut was made at 140 microns radially from the root canal space, leaving sections of about 140 microns thick. Therefore each section had a surface which was about 150 microns from the root canal and the other surface was about 290 microns from the root canal. The surface that was further away from the root canal is referred as the top surface and the surface nearer to the root canal is referred as the bottom surface in this study, for simplicity.

Further cuts were made such that the final overall dimension of each dentin piece was about 3mm by 4mm by 0.14mm. The final steps required gradual polishing. The dentin pieces were gently hand polished using 2500 grit and a final 4000 grit alumina oxide coated paper. This is to ensure a smooth surface exists for the nanoindentation tests. Figure 3-2 shows the top view of the schematic drawing of the dentin sections from the tooth (not drawn to scale).

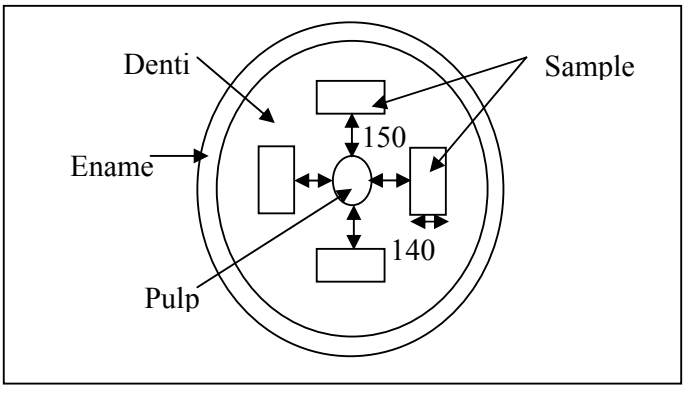

Figure 3-2: Top view of the schematic drawing of the dentin sections

A small mark was made using a red marker at the top surface of each sample. This was made to enable us to know which side is nearer to the pulp (bottom) and which side is further away (top) during imaging and nanoindentation tests. The samples are then placed in Hank's balanced salt solution.

3.2 Sample Testing

Prior to testing, a line was drawn using a pencil in the midline section of the samples. The samples were then fixed on individual glass slides using a double-sided tape at one end until the midline for stability. To level the height of the other end of the sample, a normal tape with approximately the same thickness was placed underneath the sample. The top of the sample was exposed first. Figure 3-3 shows a sample that is ready for testing.

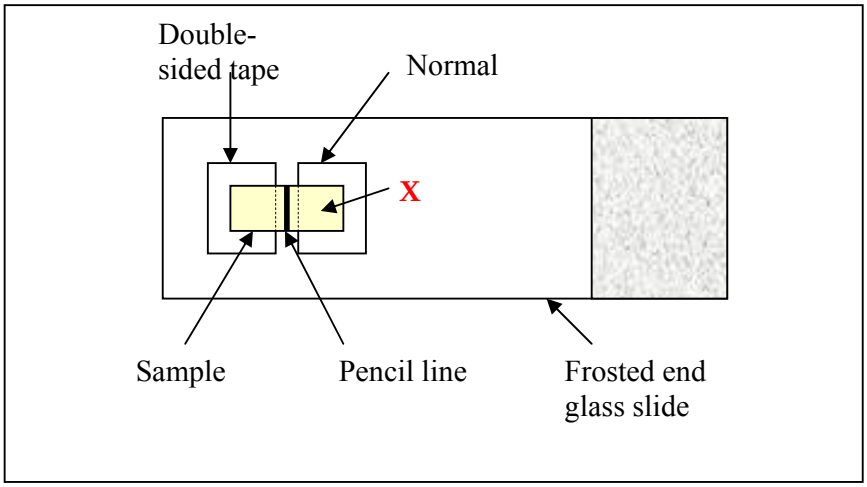

Figure 3-3: Sample mounted on glass slide

All samples were mounted as such prior to testing. The area that was tested on is the one marked as "X" in Figure 3-3. 2 AFM images using tapping mode were taken near the location. Then, the sample is flipped over to image the bottom part of the sample. Similarly, 2 AFM images were taken.

The AFM scanner head was then replaced with the Triboscope indenter system. The Berkovich tip was used in this study as it is one of the commonly used tips and worked well in this study. The tip which was previously calibrated with fused quartz, was used for imaging to select a suitable location before indentation. 10 indentations were done at location near and around "X". The baseline values for hardness and Young's modulus were automatically recorded. This baseline values will give us the mechanical properties for dentin at the bottom of the sample. Next, the sample was flipped over again. 10 indentations were done to extract its mechanical properties at the top of the sample.

The above steps give us the basic idea on how the samples were imaged and indented. For the first experiment, after the above steps, the sample was soaked for 5 minutes with EDTA. The sample was then flushed with distilled water. The experimental procedure was repeated to collect the images of the dentin as well as the mechanical properties after treatment.

Initially, the sample was supposed to be soaked in the EDTA again for 5 minutes to see whether there were any changes in the microstructure of the dentin or

mechanical properties. However, this was not possible as the sample broke into pieces after the second treatment. As such, the data collected was only for one treatment of EDTA.

The loading function for this study is shown in Figure 3-4. This loading function was chosen after several trial and error tests and it is quite similar with the study done by Kinney et al [69].

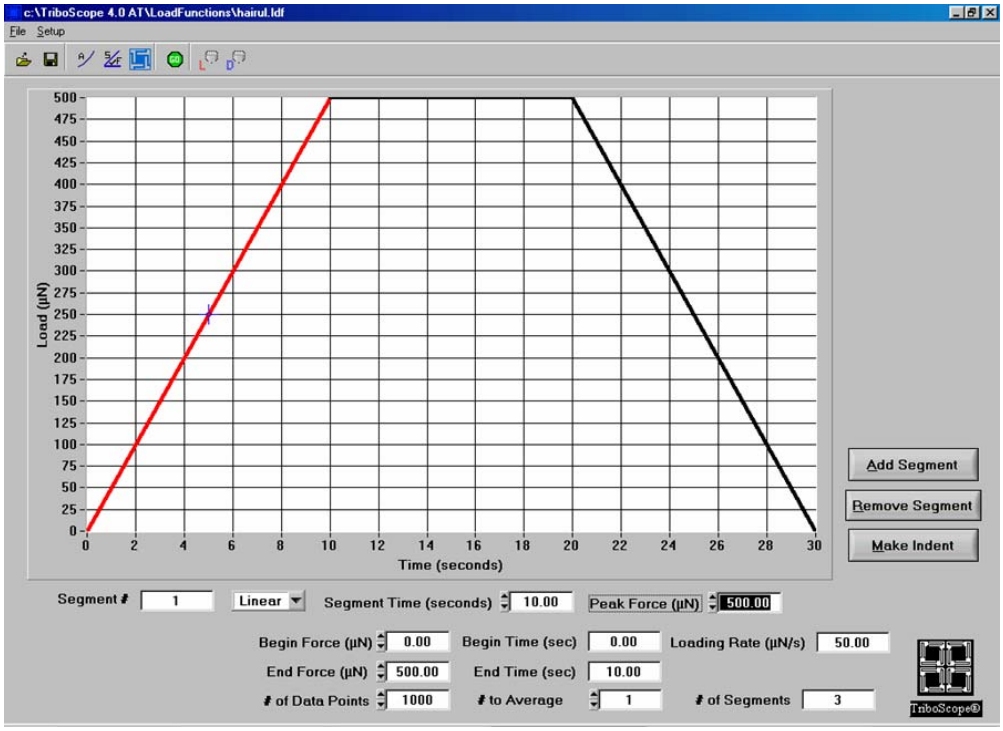

Figure 3-4: Loading function used for nanoindentation tests

With this loading function, the load was raised from 0 to 500 μN in 10 seconds. At this maximum load, the load was held for 10 seconds to eliminate the effects of creep. Finally, the load was decreased back to 0 μN in 10 seconds.

After all the data have been collected, the mean values for baseline hardness and Young's modulus were computed and compared with the mean values for hardness and Young's modulus after treatment with EDTA.

To find out the effects of NaOCl, we perform the tests similar to the one used above. We first image the top and bottom surface of the sample. Then, we used the nanoindenter to indent on the bottom and flipped over to the top to get the baseline values for both hardness and Young's modulus for the sample.

The sample was then removed and soaked in NaOCl for one hour. The samples were then flushed with distilled water. The same steps were repeated to image and indent the samples again to find the effects of NaOCl on dentin. The tests were done on all 4 samples and the same loading functions were used.

Using the Minitab 14.2, paired-sample *t*-tests were done to determine any changes in the hardness and Young's modulus before and after treatment with NaOCl. All tests were subjected to a 0.05 level of confidence.

CHAPTER 4 RESULTS AND DISCUSSION

4.1 Results on the effects of EDTA

4.1.1 AFM images

Figure 4-1 shows an AFM scan of dentin at the top while Figure 4-2 shows the bottom of the sample before any treatment with EDTA. This is the typical image obtained at various locations at the top and bottom surfaces of the sample.

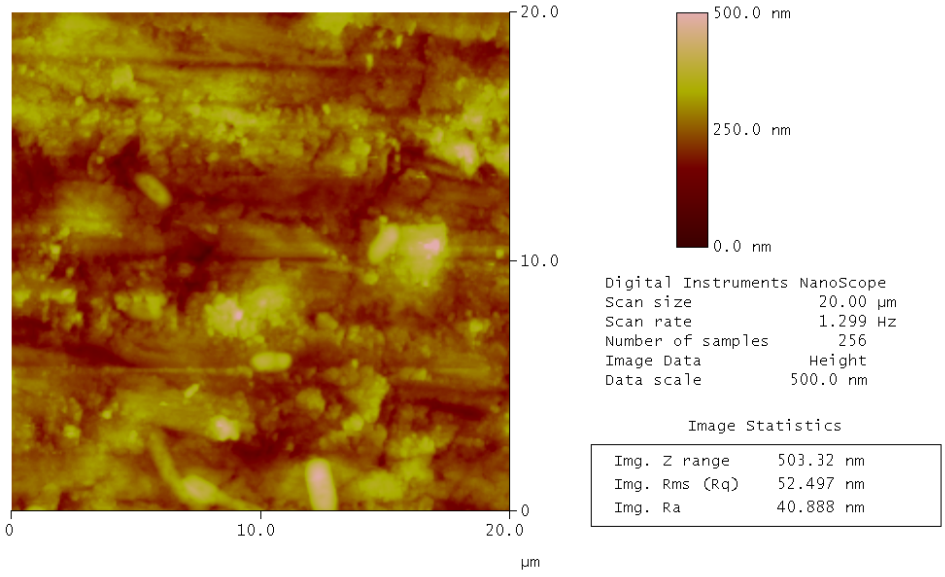

Figure 4-1: AFM scan of dentin at the top of the sample before treatment with EDTA

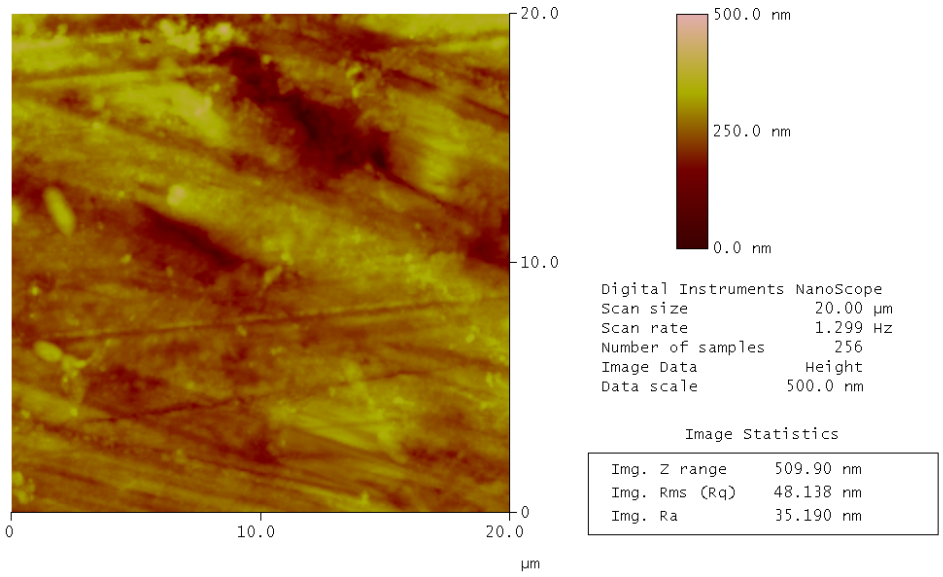

Figure 4-2: AFM scan of dentin at the bottom of the sample before treatment with EDTA

After the nanoindentation tests, the sample was then soaked in EDTA for 5 minutes and flushed with distilled water. The AFM was used again to image the top and bottom surfaces of dentin. Figure 4-3 shows the AFM scan of dentin at the top while Figure 4-4 shows the bottom of the sample.

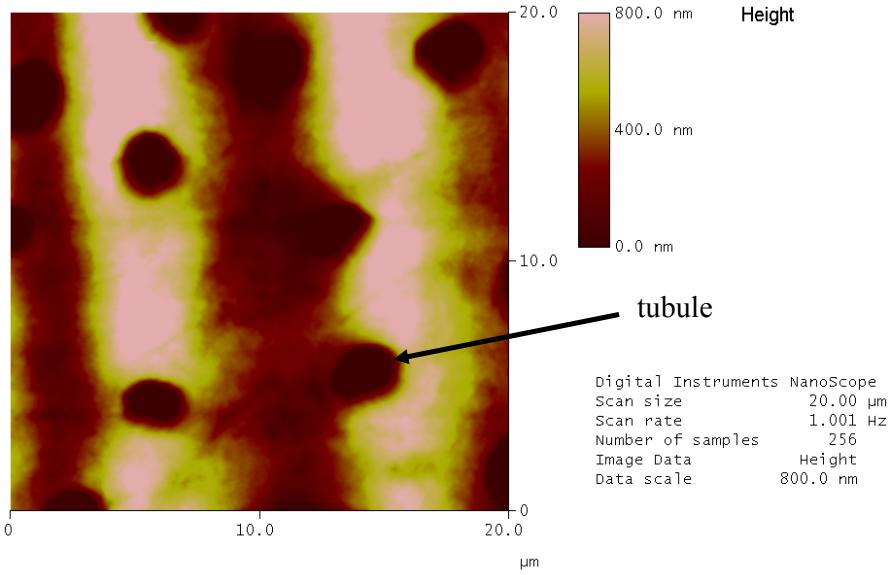

Figure 4-3: AFM scan of dentin at the top of the sample after treatment with EDTA

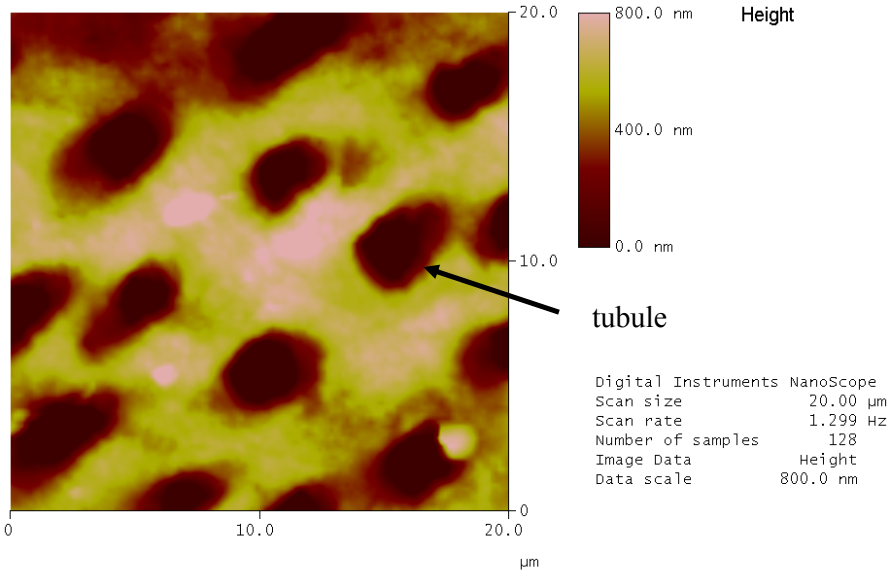

Figure 4-4: AFM scan of dentin at the bottom of the sample after treatment with EDTA

4.1.2 Nanoindentation results

The initial results were considered to be the baseline hardness and Young's modulus. The Hysitron Triboscope® software automatically calculates the hardness and Young's modulus of the samples. Other information such as the contact depth in nm, contact stiffness in μN/nm, maximum force in μN, maximum depth in nm as well as the contact area in nm^2 can also be obtained.

The calculations for the hardness and Young's modulus were based on the area tip function that was input into the software. Therefore, it is essential that the tip is calibrated after frequent usage. Figure 4-5 shows the typical force displacement curve for dentin.

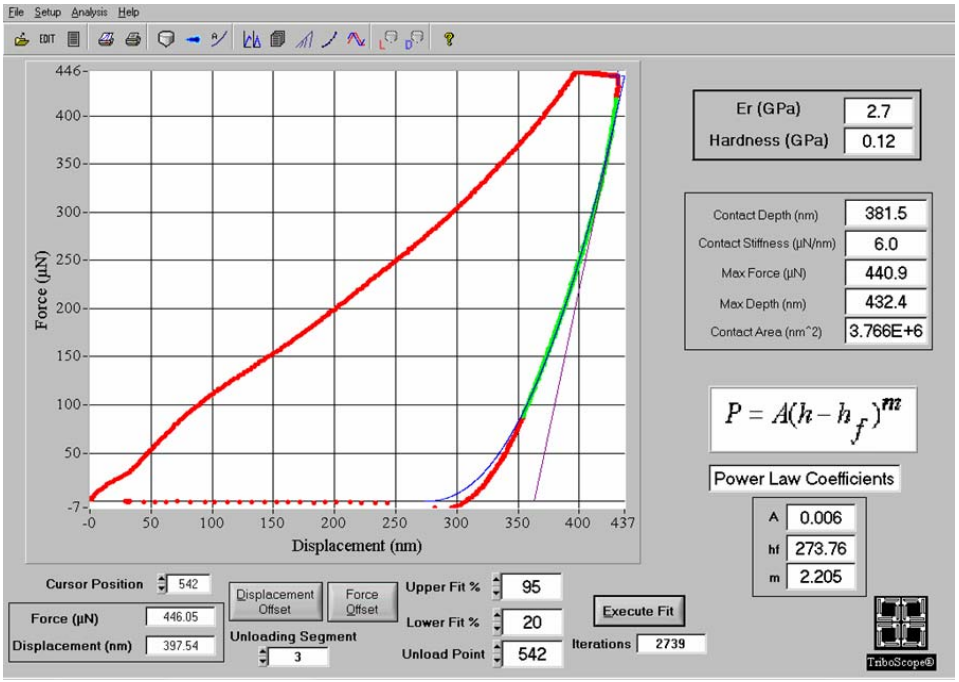

Figure 4-5: Typical force displacement curve for dentin

Even after treatment with EDTA, the force displacement curve exhibit similar characteristics as the baseline results. Only the experimental readings obtained are different.

Figure 4-6 shows an example of an indentation on dentin.

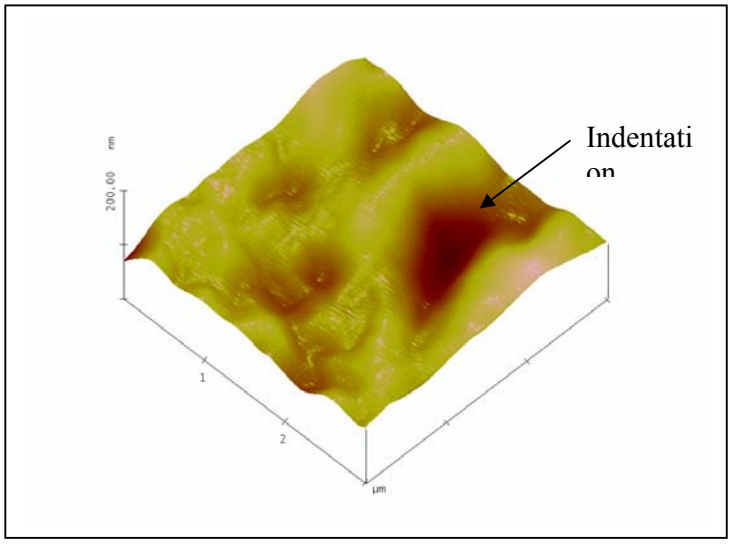

Figure 4-6: Indentation on dentin

For the baseline results, the mean Young's modulus at the bottom of the sample is 4.81 GPa and the hardness is 0.360 GPa. For the top of the sample, the mean Young's modulus is 6.91 GPa and the hardness is 0.392 GPa.

After treatment with EDTA, the mean Young's modulus at the bottom of the sample is 1.16 GPa and the hardness is 0.107 GPa. For the top of the sample, the mean Young's modulus is 1.71 GPa and the hardness is 0.116 GPa.

For a complete detail for all the individual nanoindentation results, see appendix C.

4.1.3 Statistical results

After treatment with EDTA, the mean Young's modulus for the bottom surface decreases by 76.0% while the hardness decreases by 70.2%. For the top surface, the mean Young's modulus decreases by 75.3% while the hardness decreases by 70.4%. For detailed calculations, see appendix D.

4.2 Discussions on the effects of EDTA

From the AFM images shown in Figures 4-1 and 4-2, the tubules of the dentin can hardly be seen. This is due to the smear layer that formed during the polishing of the samples. The smear layer is an amorphous boundary layer containing both mineral and organic components of dentin [70]. In cases of contamination, a bacterial component is also present in the smear layer. Both images are similar and it is difficult to distinguish the top portion and the bottom portion due to the smear layer.

After applying EDTA on the sample for 5 minutes, the smear layer was removed for both top and bottom surfaces. From Figure 4-3 and 4-4, the tubules were now clearly exposed. This shows that 17% EDTA is able to remove the smear layer after 5 minutes of application.

The main cause of this removal of smear layer was due to the demineralization of dentin. Nygard-Ostby [29] reported that with the use of 15% EDTA with an added detergent, there was 20-30 μm penetration by EDTA. This was shown by a zone of demineralization using polarized light microscopy. A 5 minutes exposure of the root canal to EDTA would remove the smear layer and open the dentinal tubules to a depth of 20-30 μm.

Kawasaki et al [71] employed neutral EDTA to remove mineral from dentin and McComb et al [72] also states that EDTA has been used effectively to remove debris from root canals.

Although most clinicians are aware of the effects of acid on dentin, the effects of EDTA on the dentin surface is not so well understood [27]. Marshall et al used AFM to show that the intertubular surface of dentin etched by phosphoric acid (3mM and 5mM) and citric acids (5mM) was smooth. However, 0.5M 17% EDTA treatment gave rise to intertubular dentin surfaces which was significantly rough.

Machado-Silveiro et al [73] used spectrophotometry to evaluate in vitro the demineralization capability of 17% EDTA after 5, 10 and 15 minutes. It is shown that there is decalcifying activity that took place although there were no significant differences in the activity between the three time periods.

There are other studies regarding the smear layer removal by EDTA [71, 74-79]. In the past, there was no specific consensus regarding the efficacy of smear layer removal in the root canal treatment [75, 77, 79]. It has been suggested that retaining the smear layer may inhibit or delay bacterial colonization of the root canal by reducing permeability. However, currently, the consensus is towards the removal of smear layer in order to reduce the microflora and associated endotoxins [76]. This is also to enhance the sealing capability of obturating materials and decrease potential of the bacteria to survive and reproduce.

Although the original study was to image the dentin again for another 5 minutes to see any visible changes, it was not possible as the sample became very brittle and breaks into pieces during handling. This study shows that dentin become much more brittle after application of EDTA.

For the baseline nanoindentation results, it can be seen that the hardness and Young's modulus of the top and bottom differs slightly. In a study by Kinney et al [17], the hardness and Young's modulus for intertubular dentin are smaller nearer to the pulp and larger away from the pulp. The values obtained here are consistent with that study as the hardness and Young's modulus of the bottom surface are smaller than the top surface.

After treatment, the demineralization of dentin by EDTA also results in the decrease in hardness and Young's modulus. This is evident from the nanoindentation and statistical results. The figures below gives a clearer view on

the effects of EDTA on the mechanical properties of dentin. Figure 4-7 shows the differences of the mean Young's modulus of the top surface after treatment while Figure 4-8 shows its hardness.

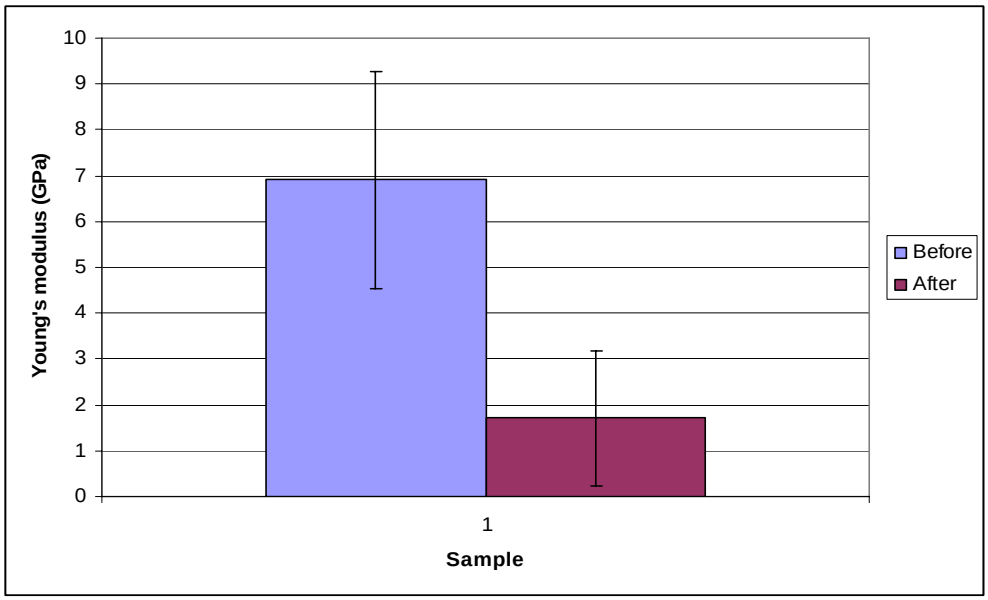

Figure 4-7: Differences in Young's modulus for top surface after EDTA treatment

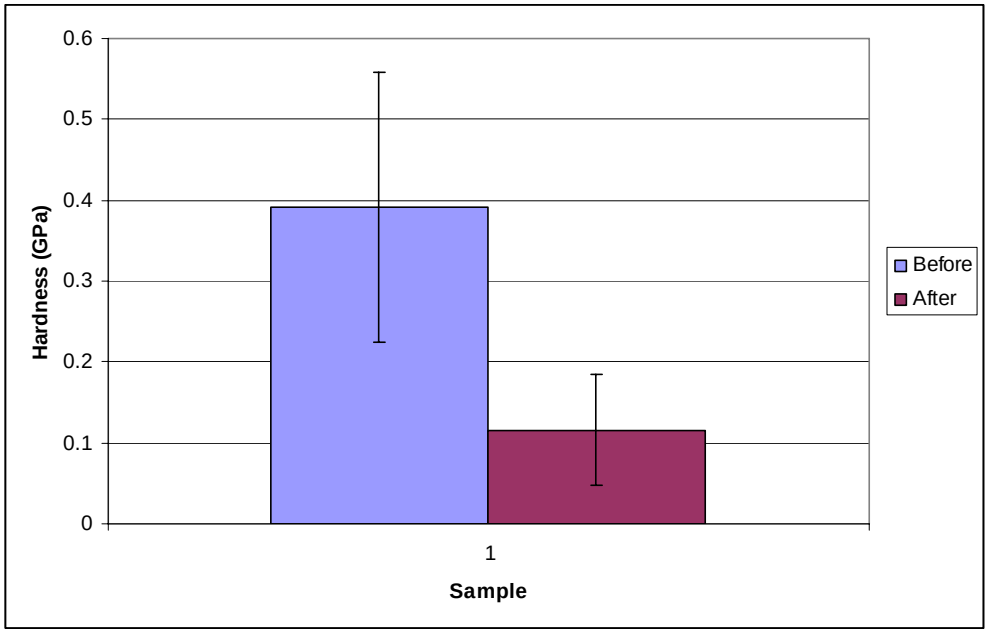

Figure 4-8: Differences in hardness for top surface after EDTA treatment

Figure 4-9 and figure 4-10 shows the differences of their mean Young's modulus and hardness of the bottom surface after treatment, respectively.

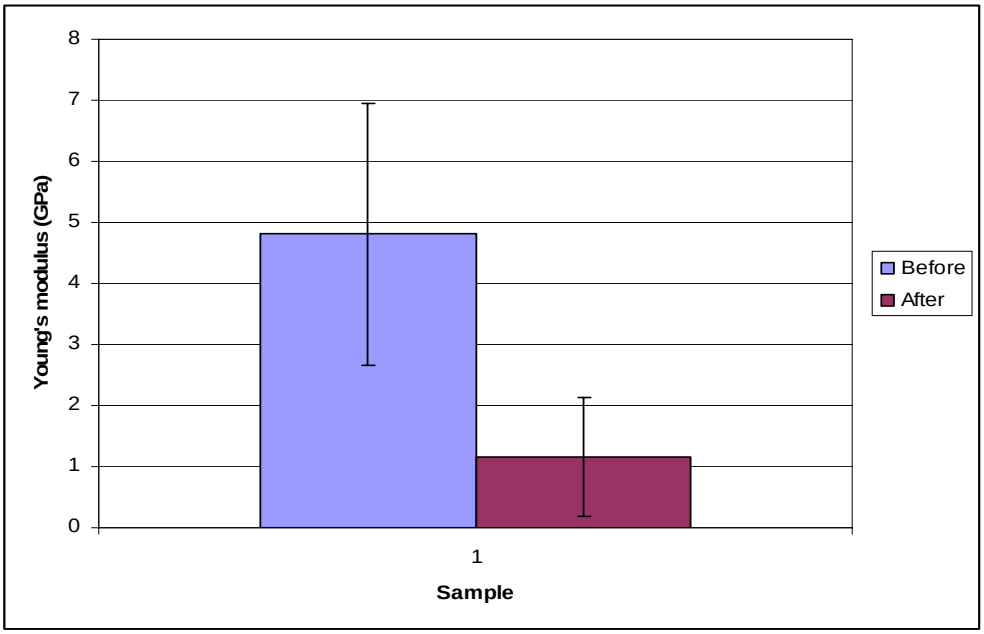

Figure 4-9: Differences in Young's modulus for bottom surface after EDTA treatment

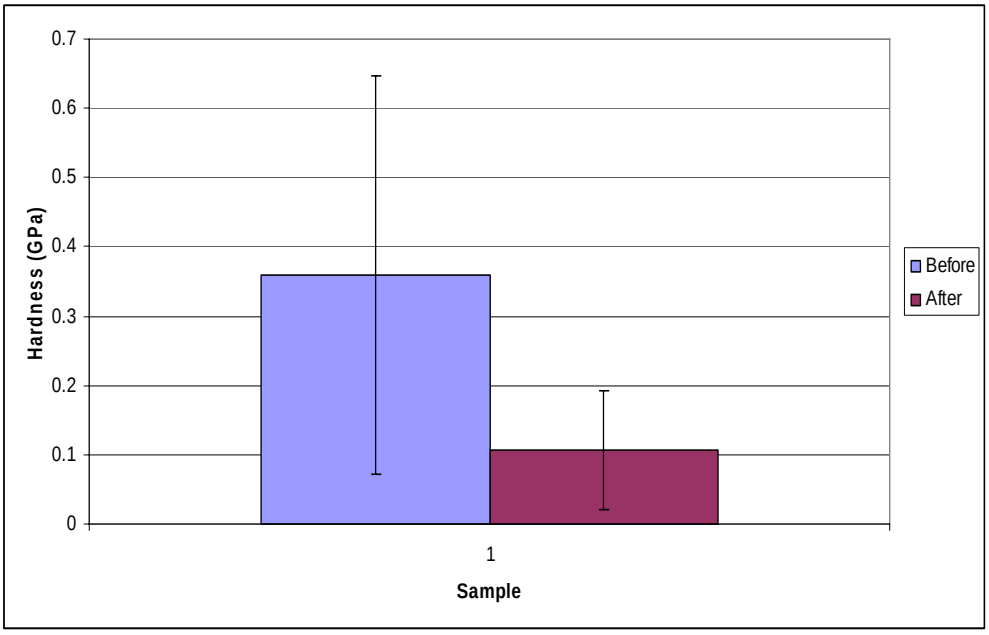

Figure 4-10: Differences in hardness for bottom surface after EDTA treatment

From the graphs, it can be seen that there is a reduction in the mechanical properties of dentin after treatment with EDTA. From the statistical results, the Young's modulus decreases by 75.3% and 76.0% for top and bottom, respectively. The hardness also decreases by 70.4% and 70.2% for the top and bottom surfaces, respectively.

The main cause for this is again due to the demineralization of the dentin. As EDTA is a decalcifying agent, the dissolution of calcium hydroxyapatite in dentin exposes the organic matrix of dentin (mostly type I collagen) [80]. This could result in the decrease of the hardness and Young's modulus of dentin.

Saleh et al [81] used a microhardness tester with a Knoop diamond indenter to study the effects of EDTA on dentin. Although using different testing methods, it was found that the microhardness of dentin treated with EDTA had significantly reduced. The study also states that EDTA induces an adverse softening potential on the calcified components of dentin and thus reduce the microhardness of dentin.

De-Deus et al [82] also used a microhardness test to evaluate the effect of EDTA, EDTAC (EDTA added to a wetting agent, Cetavlon) and citric acid, on the microhardness of tooth. He found that EDTA was the most effective in reducing dentin hardness and citric acid has the weakest effect. EDTA reacts with the calcium ions in the hydroxyapatite crystals and this process causes changes in the microstructure of dentin and changes in the calcium–phosphorus ratio. Calcium

and phosphorous present in the hydroxyapatite cystrals are the main inorganic elements of dentin. It has been indicated that microhardness determination can provide indirect evidence of mineral loss or gain in dental hard tissues [83]. Therefore, due to mineral loss, the hardness also decreases as reflected in this study.

The application of EDTA has influenced the surface roughness as seen in from the AFM images. This also could further influence the nanohardness and elasticity of the dentin [84].

Finally, it can be seen that the reduction in hardness and Young's modulus is roughly similar for the top and bottom of dentin. The reduction in mechanical properties should be more for the bottom than the top due to the increase in diameter and tubule density as the pulp is approached. However, in this experiment, this is only true for the hardness and not the Young's modulus. One of the reasons could be the thickness of 140 μm is not significant enough to register such changes.

These are just some suggestions on why the hardness and Young's modulus of dentin decreased after treatment with EDTA. The exact mechanism by which EDTA affects the mechanical properties has still yet to be fully understood.

4.3 Results of the effects of NaOCl

4.3.1 AFM images

Figure 4-11 shows an AFM scan of dentin at the top while Figure 4-12 shows the bottom of the samples before any treatment with NaOCl. The images are typical of those obtained at various locations at the top and bottom surfaces of the samples.

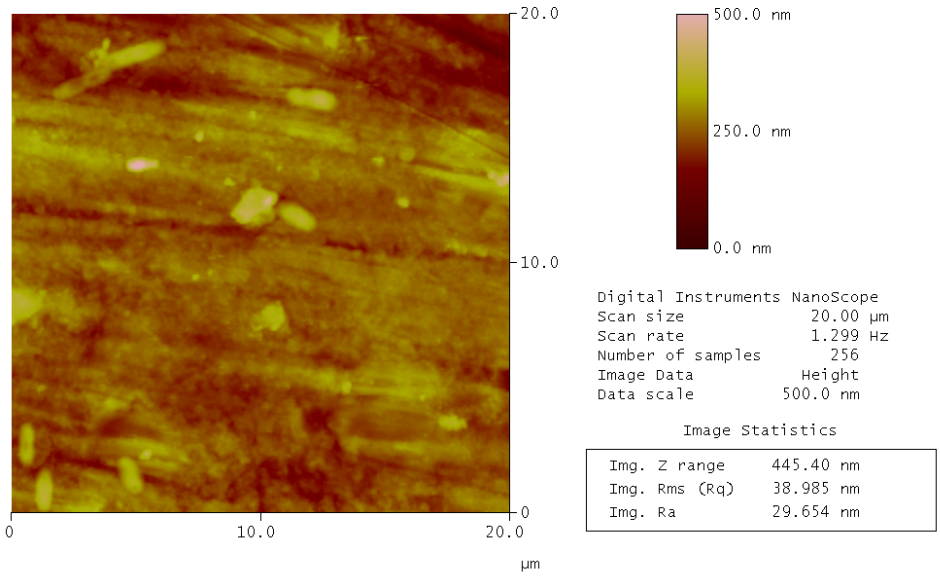

Figure 4-11: AFM scan of dentin at the top of a sample before treatment with NaOCl

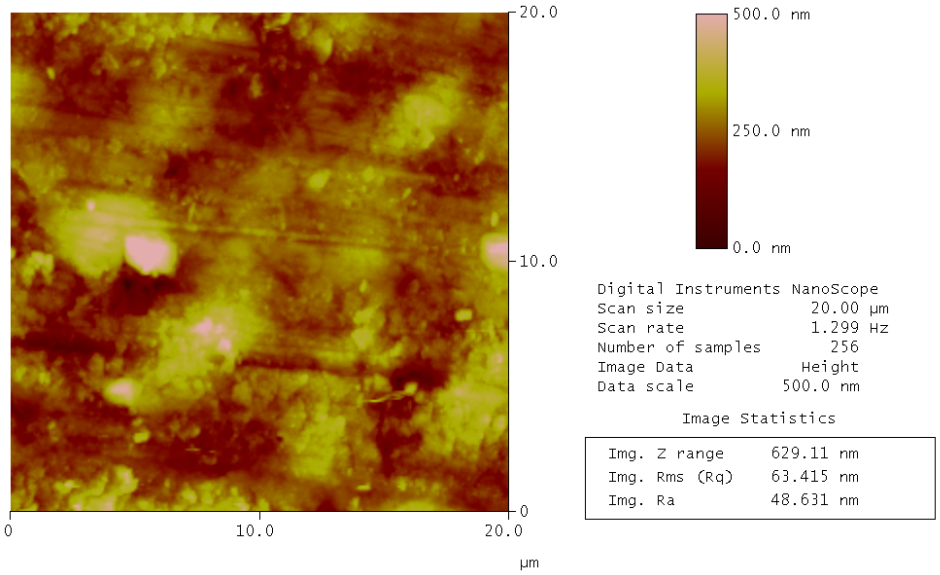

Figure 4-12: AFM scan of dentin at the bottom of a sample before treatment with NaOCl

After the nanoindentation tests, the samples were then soaked in NaOCl for 1 hour prior to imaging. The AFM was used again to image the top and bottom surfaces of the samples. Figure 4-13 shows the typical AFM scan of dentin at the top while Figure 4-14 shows the bottom of the samples.

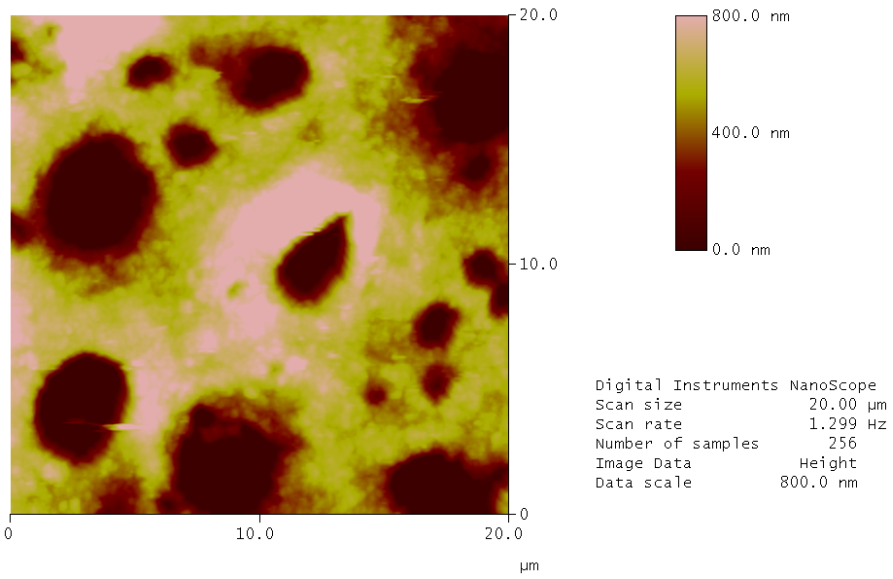

Figure 4-13: AFM scan of dentin at the top of the sample after treatment with NaOCl

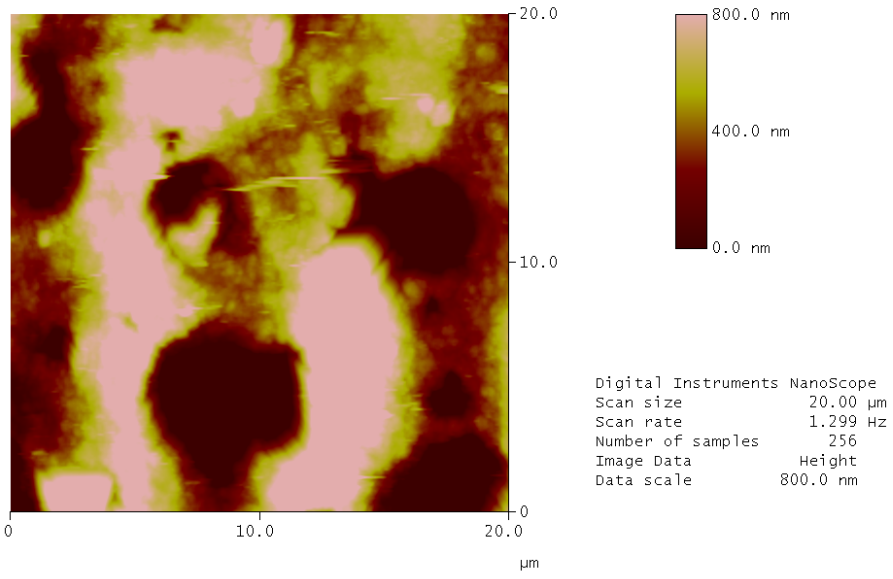

Figure 4-14: AFM scan of dentin at the bottom of the sample after treatment with NaOCl

4.3.2 Nanoindentation results

All the specimens were initially kept in Hank's balanced salt solution before the nanoindentation test to determine their baseline values for the hardness and Young's modulus. Sample 1 and 3 are obtained in the labial-buccal plane while sample 2 and 4 are obtained in the mesial-distal plane from the same tooth. Figure 4-15 shows the samples' position within the tooth.

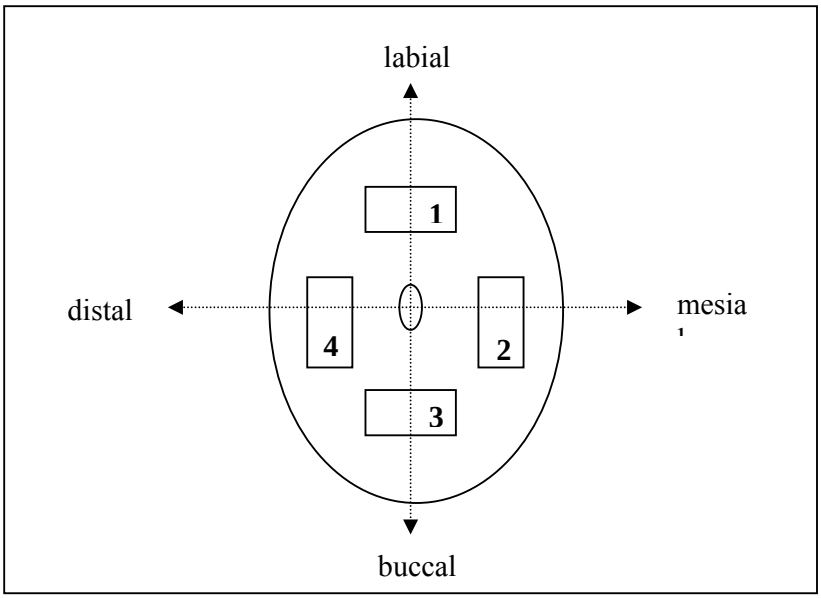

Figure 4-15: Position of samples within tooth

The force displacement curves obtained from the nanoindentation tests were similar to Figure 4-5. The values for the baseline hardness and Young's modulus were taken. Table 4-1 shows the mean baseline Young's modulus for intertubular dentin for each region while Table 4-2 shows their mean baseline hardness.

Table 4-1: Mean baseline Young's modulus of dentin

Sample No	Bottom		Top	
	Mean E (GPa)	St Dev (GPa)	Mean E (GPa)	St Dev (GPa)
1	2.63	0.68	2.61	0.51
2	2.45	0.48	2.58	1.12
3	2.75	0.53	4.27	2.60
4	3.00	0.30	4.21	2.42

Table 4-2: Mean baseline hardness of dentin

Sample No	Bottom		Top	
	Mean H (GPa)	St Dev (GPa)	Mean H (GPa)	St Dev (GPa)
1	0.167	0.055	0.193	0.114
2	0.191	0.057	0.172	0.131
3	0.223	0.095	0.175	0.067
4	0.229	0.039	0.180	0.072

After the baseline values for the hardness and Young's modulus were obtained, the specimen is soaked in 5.25% NaOCl for 1 hour prior to testing with nanoindentation again. The same number of indentations was done on approximately the same area as before. The values for Young's modulus and hardness were then recorded. Table 4-3 shows the mean Young's modulus for dentin and Table 4-4 shows their mean hardness after treatment.

Table 4-3: Mean Young's modulus dentin after treatment with 5.25% NaOCl

Sample No	Bottom		Top	
	Mean E (GPa)	St Dev (GPa)	Mean E (GPa)	St Dev (GPa)
1	0.66	0.77	1.47	0.72
2	1.86	0.75	2.34	0.59
3	1.62	0.54	2.85	1.18
4	0.89	0.40	2.74	1.75

Table 4-4: Mean hardness of dentin after treatment with 5.25% NaOCl

Sample No	Bottom		Top	
	Mean H (GPa)	St Dev (GPa)	Mean H (GPa)	St Dev (GPa)
1	0.029	0.033	0.095	0.066
2	0.093	0.055	0.143	0.043
3	0.078	0.032	0.043	0.011
4	0.036	0.014	0.062	0.018

The results for the individual indentations can be found in the Appendix E.

4.3.3 Statistical results

Paired sample *t*-tests were done using the Minitab 14.2 statistical software. The Young's modulus and hardness were compared before and after treatment with NaOCl. The top and bottom of the specimens were compared separately. All tests were done at 0.05 level of significance.

For the top surface of the specimens, there are significant changes in Young's modulus (P=0.033) as well as the hardness (P-value=0.026) after treatment. Similarly, for the bottom surface of the specimens, there are also significant changes in the Young's modulus (P-value=0.027) as well as the hardness (P-value=0.005).

The full results of the statistical analysis using Minitab 14.2 software can be found in Appendix F.

4.4 Discussions on the effects of NaOCl

From Figures 4-11 and 4-12, it can be observed that the smear layers were covering up the tubules. These two figures look identical and it is difficult to distinguish the top surface and the bottom surface due to the smear layers. Also, it can be seen that Figures 4-11 and 4-12 are similar to Figures 4-1 and 4-2. This shows that the sample preparation was similar which results in the similar phenomenon of the smear layers.

When the samples were soaked in NaOCl for 1 hour, the smear layers for each sample were removed as shown in Figures 4-13 and 4-14 for both the top and bottom surfaces.

NaOCl is known as a solution capable of modifying dentin surfaces [85-87]. It can dissolve proteins, and thus known as a deproteinating agent. Previously, NaOCl has been used to remove the organic components of biological materials [88, 89].

On teeth, NaOCl solutions are used routinely to remove organic debris from pulp canals during endodontic therapy [70]. Additionally, in some recent studies [90, 91], NaOCl was used on dentin to dissolve the collagen exposed by acid treatment. This is the reason why the smear layers were removed as smear layers are comprised of both organic and inorganic components. Removal of the organic components may also allow removal of the inorganic components.

From the nanoindentation and statistical results, it can be seen that the hardness and Young's modulus decreased after treatment with NaOCl for both the top and bottom surfaces. In this study, the Young's modulus decreased by 9.3 to 43.8% for the top surface while its hardness decreased by 17.1 to 75.2%. For the bottom surface, the Young's modulus decreased by 23.8 to 74.7% while the hardness decreased by 51.1 to 84.5% after treatment. For full calculation details, see appendix G. Figure 4-16 shows the differences in Young's modulus after treatment for the top surface while figure 4-17 shows the differences in hardness.

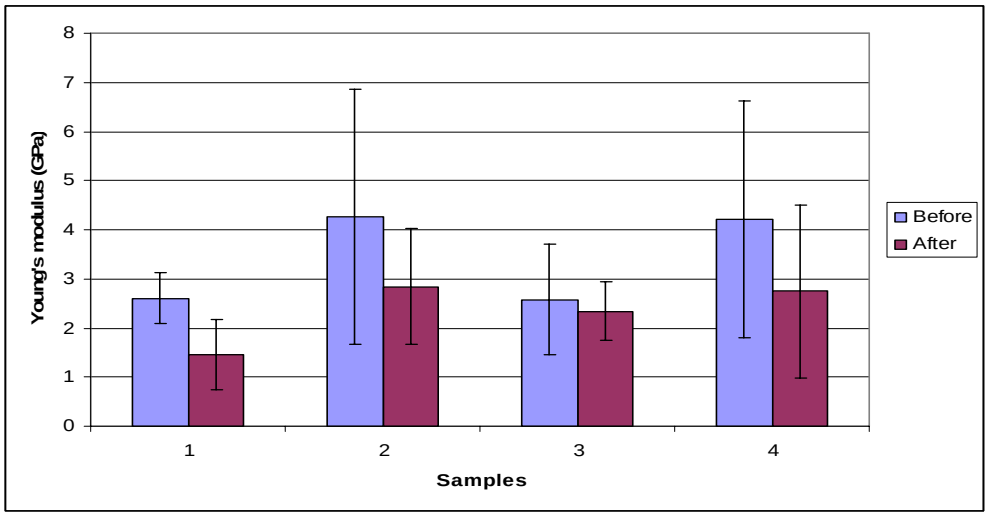

Figure 4-16: Differences in Young's modulus for top surface after NaOCl treatment

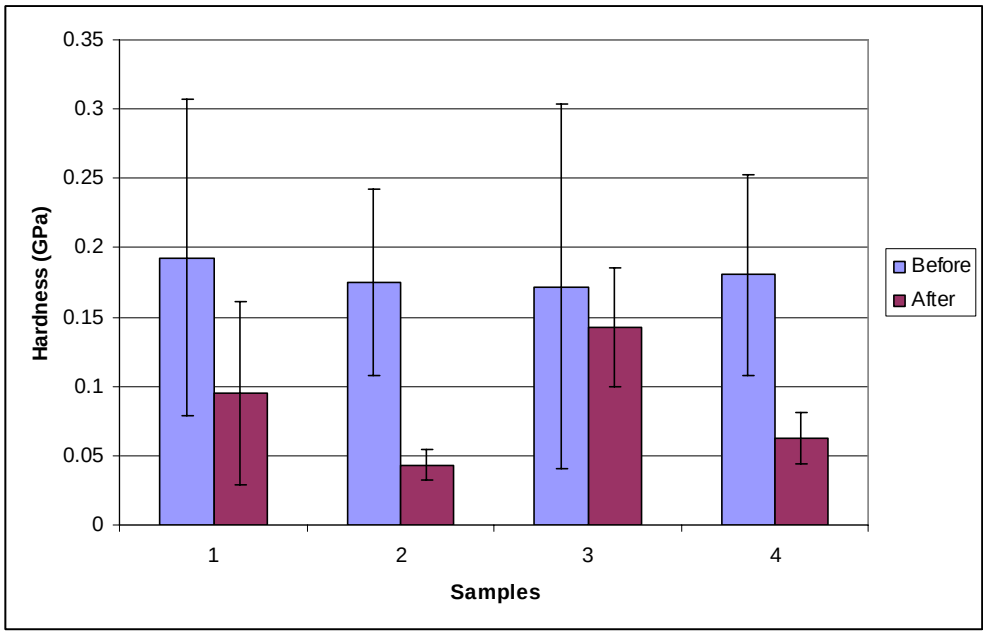

Figure 4-17: Differences in hardness for top surface after NaOCl treatment

Figure 4-18 and figure 4-19 show the differences in the Young's modulus and hardness for the bottom surface respectively.

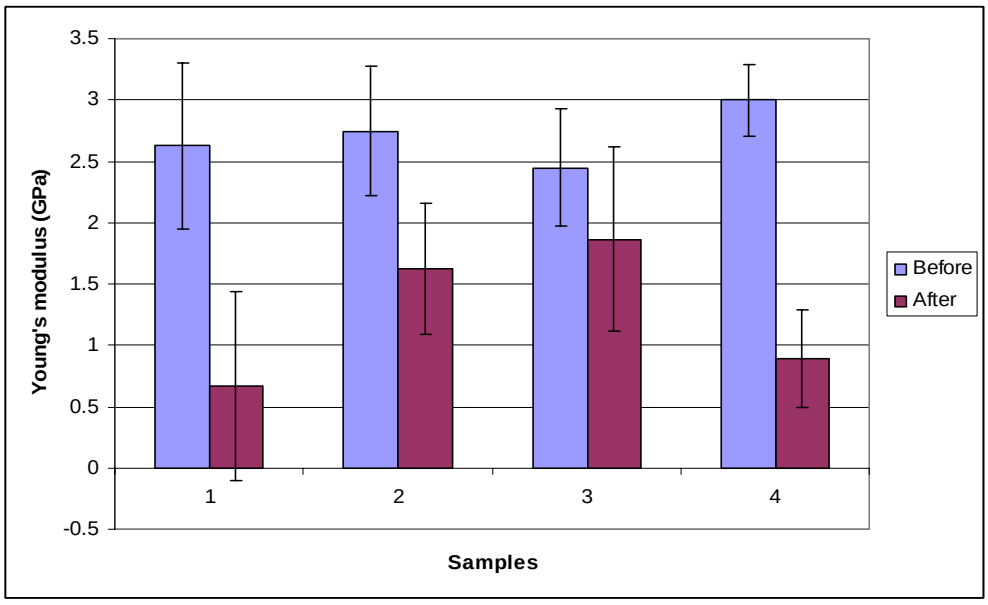

Figure 4-18: Differences in Young's modulus for bottom surface after NaOCl treatment

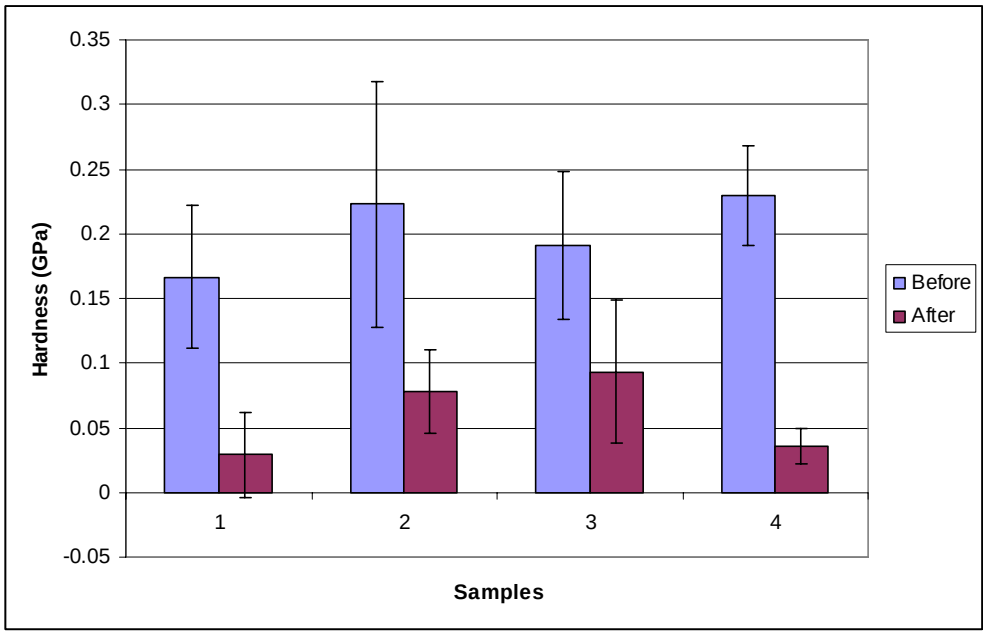

Figure 4-19: Differences in hardness for bottom surface after NaOCl treatment

The main cause of the decrease is again due to the deproteination of the dentin. The action of NaOCl involves the slow dissolution of encapsulated collagen which leaves behind the hydroxyapatite cystals [70]. After sufficient exposure, the deproteination leaves behind a very brittle material. This was why the hardness and Young's modulus decreased after treatment. This was also the reason why the some of the samples broke after treatment and further testing cannot be done.

Dentin deproteination is a relatively slow process for unexposed collagen [70]. That is why the samples are soaked much longer, for 1 hour, compared to treatment with EDTA which is only for 5 minutes.

NaOCl is a well-known non-specific proteolytic agent that is capable of removing organic material [92], as well as magnesium and carbonate ions [86]. After

treatment with NaOCl, these effects may cause the hardness and Young's modulus of the samples to decrease.

Also, from the AFM images in Figures 4-11 to 4-14, it can be seen that the surface roughness was altered. This alteration may also result in the changes of the hardness and elasticity of the dentin [84]. It is mentioned that as the surface roughness of a surface increases, the hardness measured at depths comparable with the roughness scale deviates increasingly from the actual hardness.

When we compare the decrease in hardness and Young's modulus for each sample individually, we can see that the decrease was more for the bottom surface than the top surface for almost all samples. The reasons for this could be due the increase in diameter and tubule density as the pulp is approached. As such, the bottom surface could be affected more than the top surface.

Finally, when we compare the decrease in hardness in the labial-buccal plane (samples 1 and 3) and the mesial-distal plane (samples 2 and 4), there was not much difference. This shows that NaOCl treatment affects the samples equally and not dependent on which plane they are from. The reason is probably that the surfaces of the samples were all about equidistant from the pulp.

Again, these are just suggestions on why the hardness and modulus of dentin decreased after treatment with NaOCl. The exact mechanisms by which the mechanical properties are affected still have to be fully understood.

CHAPTER 5 CONCLUSIONS

It can be seen that the AFM and nanoindenter are powerful tools that can characterize biological samples like teeth with high precision at the nanometer scale. Although sample preparation, handling and testing are difficult and time-consuming, the results can still be obtained.

In this study, with the AFM, it can be seen that smear layers were formed during sample preparation. After application of 17% EDTA for 5 minutes, the smear layers were removed. Also the mean hardness and Young's modulus decreased significantly from its baseline mechanical properties. The main reason for both behaviors is due to the demineralization of dentin by EDTA. EDTA is a decalcifying agent and reacts with calcium ions in the hydroxyapatite crystals. This process would cause changes in the microstructure of dentin and changes in the calcium-phosphorus ratio. This weakens the teeth and also caused it to be very brittle. Furthermore, the surface of the dentin was altered which could change the mechanical properties of dentin.

It was also found in this study that application of 5.25% NaOCl for 1 hour was able to remove the smear layers that were formed. However, the mean hardness and Young's modulus also decreased significantly from its baseline mechanical properties. The main cause of this would be the deproteination of dentin by NaOCl. The dissolution action of NaOCl removes the organic material of dentin. This would weaken the teeth and would cause it to be brittle. Also, the surface of

the dentin was affected by the application of the NaOCl. This would also affect the mechanical properties of dentin.

In this study, it is also found that the mechanical properties decreased in all directions which are in the mesial-distal and labial-buccal plane. There were no significant differences in the decreased mechanical properties along these 2 planes.

Although the use of these irrigants has detrimental effects on its mechanical properties, they are still very much in use in root canal treatments. Their functions are very important and cannot be compromised. This study is very practical as it provides useful information to dentist, endodontists, oral surgeons and other researchers. AFM imaging and nanoindentation can be used as a standard to study the effects of other agents on teeth. With these techniques, the best solutions and treatments can be implemented and hopefully, a better replacement for these irrigants can be found.

CHAPTER 6 RECOMMENDATIONS

From the course of this study, it is observed and recommended that the following actions be taken to improve the study on this topic or other related areas of study.

Firstly, more samples with known origin and background should be used. This can be very difficult as the teeth are obtained from clinics and mixed with other extracted teeth. Furthermore, freshly extracted samples for endodontic reasons are hard to get and given to us directly without any background information.

Secondly, the effects of EDTA treatment following NaOCl treatment can be studied. In endodontics, EDTA is sometimes used after NaOCl is used as irrigant. In this study however, most of the samples broke after the first round of treatment. Their continuing effects on the mechanical properties of teeth cannot be studied. Different protocols like a thicker prepared sample may help.

Another area that can be approached is how these irrigants affect different types of teeth such as molar, incisors and canines. This way, it can be known which types of teeth are more susceptible to these irrigants.

Finally, efforts should be made to modify the nanoindentation technique to allow more accurate measurements of the modulus and the time-dependent plastic behaviour of these hard tissues. The nanoindentation test is done mainly on metals and ceramics that are homogenous in nature. Although the technique is applied to

studies on biological samples, the absolute values might not be as accurate since they are usually non-homogenous in nature. The holding period might not eliminate the effects of creep totally. A more in-depth study such as coming up with new mechanical models for the measurements of the nanomechanical properties of these kind of samples might help in future work.

REFERENCES

1. *http://www.aae.org/patients/faqs/rootcanals.htm.*
2. *http://healthresources.caremark.com/topic/rootcanal.*
3. Marshall, G.W., Jr., Balooch, M., Kinney, J.H., and Marshall, S.J., *Atomic force microscopy of conditioning agents on dentin.* J Biomed Mater Res, 1995. **29**(11): p. 1381-7.
4. Marshall, G.W., Jr., Balooch, M., Tench, R.J., Kinney, J.H., and Marshall, S.J., *Atomic force microscopy of acid effects on dentin.* Dent Mater, 1993. **9**(4): p. 265-8.
5. Marshall, G.W., Jr., Marshall, S.J., Balooch, M., and Kinney, J.H., *Evaluating demineralization and mechanical properties of human dentin with AFM.* Methods Mol Biol, 2004. **242**: p. 141-59.
6. Finke, M., Hughes, J.A., Parker, D.M., and Jandt, K.D., *Mechanical Properties of in situ Demineralised Human Enamel Measured by AFM Nanoindentation.* Surface Science, 2001. **491**: p. 456-467.
7. Lippert, F., Parker, D.M., and Jandt, K.D., *In vitro demineralization/remineralization cycles at human tooth enamel surfaces investigated by AFM and nanoindentation.* J Colloid Interface Sci, 2004. **280**(2): p. 442-8.
8. Lippert, F., Parker, D.M., and Jandt, K.D., *Toothbrush abrasion of surface softened enamel studied with tapping mode AFM and AFM nanoindentation.* Caries Res, 2004. **38**(5): p. 464-72.
9. Kirkham, J., Brookes, S.J., Shore, R.C., Bonass, W.A., Smith, D.A., Wallwork, M.L., and Robinson, C., *Atomic force microscopy studies of*

crystal surface topology during enamel development. Connect Tissue Res, 1998. **38**(1-4): p. 91-100; discussion 139-45.

10. Marshall, G.W., Jr., Balooch, M., Gallagher, R.R., Gansky, S.A., and Marshall, S.J., *Mechanical properties of the dentinoenamel junction: AFM studies of nanohardness, elastic modulus, and fracture.* J Biomed Mater Res, 2001. **54**(1): p. 87-95.
11. Habelitz, S., Marshall, S.J., Marshall, G.W., Jr., and Balooch, M., *The functional width of the dentino-enamel junction determined by AFM-based nanoscratching.* J Struct Biol, 2001. **135**(3): p. 294-301.
12. Alguero, M., Bushby, A.J., and Reece, M.J., *Direct Measurement of Mechanical Properties of (Pb, La) TiO3 Ferroelectric Thin Films Using Nanoindentation Techniques.* Journal of Material Research, 2001. **16**: p. 993-1002.
13. Rho, J.Y., Tsui, T.Y., and Pharr, G.M., *Elastic Properties of Human Cortical and Trabecular Lamellar Bone by Nanoindentation.* Biomaterials, 1997. **35**(995-998).
14. Zysset, P.K., Guo, X.E., Hoffler, G.E., Moore, K.E., and Goldstein, S.A., *Elastic Modulus and Hardness of Cortical and Trabecular Bone Lamellae Measured by Nanoindentation In the Human Femur.* Journal of Biomechanics, 1999. **32**: p. 1005-1012.
15. Cuy, J.L., Mann, A.B., Livi, K.J., Teaford, M.F., and Weihs, T.P., *Nanoindentation mapping of the mechanical properties of human molar tooth enamel.* Arch Oral Biol, 2002. **47**(4): p. 281-91.

16. Habelitz, S., Marshall, G.W., Jr., Balooch, M., and Marshall, S.J., *Nanoindentation and storage of teeth.* J Biomech, 2002. **35**(7): p. 995-8.

17. Kinney, J.H., Balooch, M., Marshall, S.J., Marshall, G.W., Jr., and Weihs, T.P., *Hardness and Young's modulus of human peritubular and intertubular dentine.* Arch Oral Biol, 1996. **41**(1): p. 9-13.

18. Mahoney, E., Holt, A., Swain, M., and Kilpatrick, N., *The hardness and modulus of elasticity of primary molar teeth: an ultra-micro-indentation study.* J Dent, 2000. **28**(8): p. 589-94.

19. *http://www.nlm.nih.gov/medlineplus/ency/imagepages/1121.htm*.

20. Berkovitz, B.K.B., Holland, G.R., and Moxham, B.J., *Oral Anatomy: Histology and Embryology.* Mosby-Wolfe, 1977: p. 112-149.

21. Ten Cate, A.R., *Oral Histology: Development, Structure and Function.* 4th edition. St. Louis, Mosby, 1994.

22. *http://www.udp.org.uk/articles/treatments/RootCanal.html*.

23. Hui, K.C., Chen, N.N., Koh, E.T., Lam, E.C., Lim, K.C., and Sum, C.P., *Guidelines for root canal treatment.* Singapore Dent J, 2004. **26**(1): p. 60-2.

24. Perez, F. and Rouqueyrol-Pourcel, N., *Effect of a low-concentration EDTA solution on root canal walls: A scanning electron microscopic study.* Oral Surgery Oral Medicine Oral Pathology Oral Radiology and Endodontics, 2005. **99**(3): p. 383-387.

25. O'Connell, M.S., Morgan, L.A., Beeler, W.J., and Baumgartner, J.C., *A comparative study of smear layer removal using different salts of EDTA.* J Endod, 2000. **26**(12): p. 739-43.

26. Torabinejad, M., Handysides, R., Khademi, A.A., and Bakland, L.K., *Clinical implications of the smear layer in endodontics: a review.* Oral Surg Oral Med Oral Pathol Oral Radiol Endod, 2002. **94**(6): p. 658-66.

27. Sum, C.P., Neo, J., and Kishen, A., *What we leave behind in root canals after endodontic treatment: some issues and concerns.* Aust Endod J, 2005. **31**(3): p. 94-100.

28. Calt, S. and Serper, A., *Time-dependent effects of EDTA on dentin structures.* J Endod, 2002. **28**(1): p. 17-9.

29. Nygaard-Ostby, B., *Chelation in root canal therapy: ethylenediaminetetraacetic acid for cleansing and widening of root canals.* Odontologisk Tidskrift, 1957. **65**: p. 3-11.

30. Qualtrough, A.J., Whitworth, J.M., and Dummer, P.M., *Preclinical endodontology: an international comparison.* Int Endod J, 1999. **32**(5): p. 406-14.

31. Senia, E.S., Marshall, F.J., and Rosen, S., *The solvent action of sodium hypochlorite on pulp tissue of extracted teeth.* Oral Surg Oral Med Oral Pathol, 1971. **31**(1): p. 96-103.

32. Shih, M., Marshall, F.J., and Rosen, S., *The bactericidal efficiency of sodium hypochlorite as an endodontic irrigant.* Oral Surg Oral Med Oral Pathol, 1970. **29**: p. 613-619.

33. Berber, V.B., Gomes, B.P., Sena, N.T., Vianna, M.E., Ferraz, C.C., Zaia, A.A., and Souza-Filho, F.J., *Efficacy of various concentrations of NaOCl and instrumentation techniques in reducing Enterococcus faecalis within root canals and dentinal tubules.* Int Endod J, 2006. **39**(1): p. 10-7.

34. Binnig, G., Quate, C.F., and Gerber, C.H., *Atomic force microscope.* Physical Review Letters, 1986. **56**: p. 930-933.

35. Xu, H.H., Smith, D.T., Jahanmir, S., Romberg, E., Kelly, J.R., Thompson, V.P., and Rekow, E.D., *Indentation damage and mechanical properties of human enamel and dentin.* J Dent Res, 1998. **77**(3): p. 472-80.

36. *http://www.nanoscience.com/education/AFM.html*.

37. Butt, H.J., Wolff, E.K., Gould, S.A., Dixon Northern, B., Peterson, C.M., and Hansma, P.K., *Imaging cells with the atomic force microscope.* J Struct Biol, 1990. **105**(1-3): p. 54-61.

38. Li, A., Mansoor, A.H., Tan, K.S., and Lim, C.T., *Observations on the internal and surface morphology of malaria infected blood cells using optical and atomic force microscopy.* J Microbiol Methods, 2006. **66**(3): p. 434-9.

39. Radmacher, M., Tillamnn, R.W., Fritz, M., and Gaub, H.E., *From molecules to cells: imaging soft samples with the atomic force microscope.* Science, 1992. **257**(5078): p. 1900-5.

40. Zachee, P., Boogaerts, M., Snauwaert, J., and Hellemans, L., *Imaging uremic red blood cells with the atomic force microscope.* Am J Nephrol, 1994. **14**(3): p. 197-200.

41. Zachee, P., Snauwaert, J., Vandenberghe, P., Hellemans, L., and Boogaerts, M., *Imaging red blood cells with the atomic force microscope.* Br J Haematol, 1996. **95**(3): p. 472-81.

42. Lal, R., *Imaging molecular structure of channels and receptors with an atomic force microscope.* Scanning Microsc Suppl, 1996. **10**: p. 81-95; discussion 95-6.

43. Li, G., Xi, N., and Wang, D.H., *Probing membrane proteins using atomic force microscopy.* J Cell Biochem, 2006. **97**(6): p. 1191-7.

44. Muller, D.J., Janovjak, H., Lehto, T., Kuerschner, L., and Anderson, K., *Observing structure, function and assembly of single proteins by AFM.* Prog Biophys Mol Biol, 2002. **79**(1-3): p. 1-43.

45. Pera, I., Stark, R., Kappl, M., Butt, H.J., and Benfenati, F., *Using the atomic force microscope to study the interaction between two solid supported lipid bilayers and the influence of synapsin I.* Biophys J, 2004. **87**(4): p. 2446-55.

46. Hassenkam, T., Fantner, G.E., Cutroni, J.A., Weaver, J.C., Morse, D.E., and Hansma, P.K., *High-resolution AFM imaging of intact and fractured trabecular bone.* Bone, 2004. **35**(1): p. 4-10.

47. Hassenkam, T., Jorgensen, H.L., and Lauritzen, J.B., *Mapping the imprint of bone remodeling by atomic force microscopy.* Anat Rec A Discov Mol Cell Evol Biol, 2006. **288**(10): p. 1087-94.

48. Wiesmann, H.P., Chi, L., Stratmann, U., Plate, U., Fuchs, H., Joos, U., and Hohling, H.J., *Sutural mineralization of rat calvaria characterized by atomic-force microscopy and transmission electron microscopy.* Cell Tissue Res, 1998. **294**(1): p. 93-7.

49. Balooch, G., Marshall, G.W., Marshall, S.J., Warren, O.L., Asif, S.A., and Balooch, M., *Evaluation of a new modulus mapping technique to*

investigate microstructural features of human teeth. J Biomech, 2004. **37**(8): p. 1223-32.

50. De-Deus, G., Paciornik, S., Pinho Mauricio, M.H., and Prioli, R., *Real-time atomic force microscopy of root dentine during demineralization when subjected to chelating agents.* Int Endod J, 2006. **39**(9): p. 683-92.

51. El Feninat, F., Ellis, T.H., Sacher, E., and Stangel, I., *A tapping mode AFM study of collapse and denaturation in dentinal collagen.* Dent Mater, 2001. **17**(4): p. 284-8.

52. Farina, M., Schemmel, A., Weissmuller, G., Cruz, R., Kachar, B., and Bisch, P.M., *Atomic force microscopy study of tooth surfaces.* J Struct Biol, 1999. **125**(1): p. 39-49.

53. Marshall, G.W., Jr., Chang, Y.J., Gansky, S.A., and Marshall, S.J., *Demineralization of caries-affected transparent dentin by citric acid: an atomic force microscopy study.* Dent Mater, 2001. **17**(1): p. 45-52.

54. Marshall, G.W., Jr., Chang, Y.J., Saeki, K., Gansky, S.A., and Marshall, S.J., *Citric acid etching of cervical sclerotic dentin lesions: an AFM study.* J Biomed Mater Res, 2000. **49**(3): p. 338-44.

55. Chng, H.K., Ramli, H.N., Yap, A.U.J., and Lim, C.T., *Effect of hydrogen peroxide on intertubular dentine.* Journal of Dentistry, 2005. **33**(5): p. 363-369.

56. Ho, S.P., Goodis, H., Balooch, M., Nonomura, G., Marshall, S.J., and Marshall, G., *The effect of sample preparation technique on determination of structure and nanomechanical properties of human cementum hard tissue.* Biomaterials, 2004. **25**(19): p. 4847-4857.

57. http://www.hysitron.com/PDF/0312-001%20Tip%20Guide.pdf.

58. Hairul Nizam, B.R. and Lim, C.T., *Nanoindentation of Teeth - A Review.* Journal of Experimental Mechanics, 2006. **21**(1): p. 35-50.

59. Oliver, W.C. and Pharr G.M., *An Improved Technique for Determining Hardness and Elastic Modulus Using Load and Displacement Sensing Indentation Experiments.* Journal of Materials Research, 1992. **7**: p. 1564-1583.

60. Hairul Nizam, B.R., Lim, C.T., Chng, H.K., and Yap, A.U., *Nanoindentation study of human premolars subjected to bleaching agent.* J Biomech, 2005. **38**(11): p. 2204-11.

61. Pashley, D., Okabe, A., and Parham, P., *The Relationship Between Dentin Microhardness and Tubule Density.* Endo. Dent. Traumatol, 1985. **1**: p. 176-179.

62. Habelitz, S., Marshall, S.J., Marshall, G.W., Jr., and Balooch, M., *Mechanical properties of human dental enamel on the nanometre scale.* Arch Oral Biol, 2001. **46**(2): p. 173-83.

63. Angker, L., Nockolds, C., Swain, M.V., and Kilpatrick, N., *Correlating the mechanical properties to the mineral content of carious dentine--a comparative study using an ultra-micro indentation system (UMIS) and SEM-BSE signals.* Arch Oral Biol, 2004. **49**(5): p. 369-78.

64. Angker, L., Swain, M.V., and Kilpatrick, N., *Characterising the micro-mechanical behaviour of the carious dentine of primary teeth using nano-indentation.* J Biomech, 2005. **38**(7): p. 1535-42.

65. Mahoney, E., Beattie, J., Swain, M., and Kilpatrick, N., *Preliminary in vitro assessment of erosive potential using the ultra-micro-indentation system.* Caries Res, 2003. **37**(3): p. 218-24.

66. Urabe, I., Nakajima, S., Sano, H., and Tagami, J., *Physical properties of the dentin-enamel junction region.* Am J Dent, 2000. **13**(3): p. 129-35.

67. Craig, R.G. and Peyton, F.A., *Elastic and mechanical properties of human dentin.* J Dent Res, 1958. **37**(4): p. 710-8.

68. Jantarat, J., Palamara, J.E., Lindner, C., and Messer, H.H., *Time-dependent properties of human root dentin.* Dent Mater, 2002. **18**(6): p. 486-93.

69. Kinney, J.H., Balooch, M., Marshall, G.W., and Marshall, S.J., *A micromechanics model of the elastic properties of human dentine.* Arch Oral Biol, 1999. **44**(10): p. 813-22.

70. Di Renzo, M., Ellis, T.H., Sacher, E., and Stangel, I., *A photoacoustic FTIRS study of the chemical modifications of human dentin surfaces: II. Deproteination.* Biomaterials, 2001. **22**(8): p. 793-7.

71. Kawasaki, K., Ruben, J., Stokroos, I., Takagi, O., and Arends, J., *The remineralization of EDTA-treated human dentine.* Caries Res, 1999. **33**(4): p. 275-80.

72. McComb, D. and Smith, D.C., *A preliminary scanning electron microscopic study of root canals after endodontic procedures.* J Endod, 1975. **1**(7): p. 238-42.

73. Machado-Silveiro, L.F., Gonzalez-Lopez, S., and Gonzalez-Rodriguez, M.P., *Decalcification of root canal dentine by citric acid, EDTA and sodium citrate.* Int Endod J, 2004. **37**(6): p. 365-9.

74. Calt, S. and Serper, A., *Smear layer removal by EGTA.* J Endod, 2000. **26**(8): p. 459-61.

75. Cergneux, M., Ciucchi, B., Dietschi, J.M., and Holz, J., *The influence of the smear layer on the sealing ability of canal obturation.* Int Endod J, 1987. **20**(5): p. 228-32.

76. Di Lenarda, R., Cadenaro, M., and Sbaizero, O., *Effectiveness of 1 mol L-1 citric acid and 15% EDTA irrigation on smear layer removal.* Int Endod J, 2000. **33**(1): p. 46-52.

77. Gettleman, B.H., Messer, H.H., and ElDeeb, M.E., *Adhesion of sealer cements to dentin with and without the smear layer.* J Endod, 1991. **17**(1): p. 15-20.

78. Kokkas, A.B., Boutsioukis, A., Vassiliadis, L.P., and Stavrianos, C.K., *The influence of the smear layer on dentinal tubule penetration depth by three different root canal sealers: an in vitro study.* J Endod, 2004. **30**(2): p. 100-2.

79. Sen, B.H., Wesselink, P.R., and Turkun, M., *The smear layer: a phenomenon in root canal therapy.* Int Endod J, 1995. **28**(3): p. 141-8.

80. Di Renzo, M., Ellis, T.H., Sacher, E., and Stangel, I., *A photoacoustic FTIRS study of the chemical modifications of human dentin surfaces: I. Demineralization.* Biomaterials, 2001. **22**(8): p. 787-92.

81. Saleh, A.A. and Ettman, W.M., *Effect of endodontic irrigation solutions on microhardness of root canal dentine.* J Dent, 1999. **27**(1): p. 43-6.

82. De-Deus, G., Paciornik, S., and Mauricio, M.H.P., *Evaluation of the effect of EDTA, EDTAC and citric acid on the microhardness of root dentine.* International Endodontic Journal, 2006. **39**(5): p. 401-407.

83. Arends, J. and ten Bosch, J.J., *Demineralization and remineralization evaluation techniques.* J Dent Res, 1992. **71 Spec No**: p. 924-8.

84. Bobji, M.S. and Biswas, S.K., *Estimation of Hardness by Nanoindentation of Rough Surfaces.* Journal Material Research, 1998. **13**: p. 3227-3233.

85. Calas, P., Rochd, T., and Michel, G., *In vitro attachment of Streptococcus sanguis to the dentin of the root canal.* J Endod, 1994. **20**(2): p. 71-4.

86. Sakae, T., Mishima, H., and Kozawa, Y., *Changes in bovine dentin mineral with sodium hypochlorite treatment.* J Dent Res, 1988. **67**(9): p. 1229-34.

87. Zach, A. and Kaufman, A.Y., *Quantitative evaluation of the influence of dequalinium acetate and sodium hypochlorite on human dentition.* Oral Surg Oral Med Oral Pathol, 1983. **55**(5): p. 524-6.

88. Nakamura, H., Asai, K., Fujita, H., Nakazato, H., Nishimura, Y., Furuse, Y., and Sahashi, E., *The solvent action of sodium hypochlorite on bovine tendon collagen, bovine pulp, and bovine gingiva.* Oral Surg Oral Med Oral Pathol, 1985. **60**(3): p. 322-6.

89. Schiller, J., Arnhold, J., and Arnold, K., *NMR studies of the action of hypochlorous acid on native pig articular cartilage.* Eur J Biochem, 1995. **233**(2): p. 672-6.

90. Gwinnett, A.J., *Altered tissue contribution to interfacial bond strength with acid conditioned dentin.* Am J Dent, 1994. **7**(5): p. 243-6.

91. Wakabayashi, Y., Kondou, Y., Suzuki, K., Yatani, H., and Yamashita, A., *Effect of dissolution of collagen on adhesion to dentin.* Int J Prosthodont, 1994. **7**(4): p. 302-6.

92. Inaba, D., Ruben, J., Takagi, O., and Arends, J., *Effect of sodium hypochlorite treatment on remineralization of human root dentine in vitro.* Caries Res, 1996. **30**(3): p. 218-24.

93. Huo, B., *An inhomogeneous and anisotropic constitutive model of human dentin.* J Biomech, 2005. **38**(3): p. 587-94.

APPENDIX A CALCULATION OF HARDNESS, H

Tip calibration is based on determining the area function. The assumption of this method is that the Young's modulus is independent of indentation depth. Fused quartz with Young's modulus of 69 GPa is used as a standard sample for calibration purpose. An area function relating the projected contact area (A) to the contact depth is obtained. For a new and ideal Berkovich tip, the projected area to depth is given by

$$A = 24.5h_c^{\,2} \qquad \text{(A.1)}$$

However after frequent use, the ideal geometry of the tip is no longer applicable due to the blunting of the tip. The use of ideal geometry will overestimate the hardness and modulus at small depths. Therefore for a real indenter, the cross-sectional area is represented as a function of the distance from its tip. If this contact depth, h_c, is obtained from the load-displacement data, the contact area, A_c can be estimated from the area function

$$A(h_c) = 24.5h_c^{\,2} + C_1h_c^{\,1} + C_2h_c^{\,1/2} + C_3h_c^{\,1/4} + ... + C_8h_c^{\,1/128} \qquad \text{(A.2)}$$

where C_1 through C_8 are constants. As seen earlier, the leading term describes the perfect shape of the Berkovich indenter. The other terms describes deviations

from the Berkovich geometry. The Triboscope® software can be used to conveniently fit the curve to give a good area function.

The hardness, H, is then simply defined as equation A.3

$$H = \frac{W_{\max}}{A_c} \tag{A.3}$$

where $W_{\max}$ is the maximum applied load and A_c the contact area in equation A.2.

APPENDIX B CALCULATION OF YOUNG'S MODULUS, E

The elastic modulus can be obtained from the initial slope of the unloading curve (dW/dh) where it is assumed to be elastic displacement of the specimen. Analysis by Oliver et al [15] shows that the unloading data could be accurately defined as

$$W = \alpha(h - h_f)^m \tag{B.1}$$

where, W is the indenter load, h the penetration depth, h_f the final unloading depth, α contains geometric constants and m is a power law exponent related to the geometry of the indenter.

Oliver et al **[15]** proposed the use of the power law relation (B.1) to curve fit the unloading data. α, m are constants determined from the fitting procedure. The initial unloading slope is found analytically by differentiating (B.1) and evaluating it at the maximum loading point ($h_{\max}, W_{\max}$). Assuming that the initial unloading is purely elastic, the slope, also known as contact stiffness, S is given by

$$S = \frac{dW}{dh} = \frac{2\beta}{\sqrt{\pi}} E_r \sqrt{A_c} \tag{B.2}$$

where, β =1.034 for a triangular punch, E_r is the reduced modulus and A_c the contact area (A.2).

$$E_r = \frac{\sqrt{\pi}}{2\sqrt{A_{\max}}} \frac{dW}{dh} \tag{B.3}$$

where, E_r, which accounts for deformation of both sample and indenter can be determined. The elastic modulus, E_s of the specimen is found using (B.4).

$$\frac{1}{E_r} = \frac{1-\nu_i^2}{E_i} + \frac{1-\nu_s^2}{E_s} \tag{B.4}$$

where E_i=1140 GPa (diamond indenter) and ν_i =0.07 (diamond indenter).

Since the elastic modulus E_i is very large, the term $\frac{1-\upsilon_i^{\,2}}{E_i}$ in (B.4) tends to zero. Thus making E_s the subject, equation (10) becomes

$$E_s = E_r(1-\upsilon_s^{\,2}) \tag{B.5}$$

There are no experimental values for Poisson ratio of dentin and it is assumed to be 0.3 [93]. This means that E_s = 0.91 E_r Therefore, the error would be approximately ± 9 %. In nanoindentation tests, it is common to use E_s to be approximate to E_r as the Poisson ratio of the material is not always known.

APPENDIX C NANOINDENTATION RESULTS FOR EDTA TREATMENT

1) Table C-1: Results for dentin before treatment with EDTA

File	hc(nm)	Pmax(μN)	S(μN/nm)	A(nm^2)	hmax(nm)	heff(nm)	Er(GPa)	H(GPa)	A	hf(nm)	m
b-1.hys	292.2923	469.5234	14.88445	2263866	314.1652	315.9507	8.764804	0.207399	0.011024	238.619	2.451507
b-10.hys	270.0769	456.6671	9.638295	1949945	302.0812	305.6123	6.115385	0.234195	0.000632	174.515	2.766904
b-2.hys	224.7406	459.6501	5.157552	1383609	293.9729	291.5819	3.884827	0.332211	2.392675	190.1405	1.138234
b-3.hys	251.1517	464.7831	4.524902	1701417	326.1753	328.1893	3.073538	0.273174	0.67779	191.7379	1.328424
b-4.hys	303.5148	445.8518	4.525836	2431566	375.6908	377.3992	2.571524	0.18336	0.171739	223.5993	1.561221
b-5.hys	267.1648	448.8726	3.916313	1910572	351.3788	353.1269	2.510328	0.234941	0.311016	189.551	1.427164
b-6.hys	115.538	466.1806	3.555951	426733.1	215.05	213.8621	4.822946	1.092441	2.669965	76.39586	1.04857
b-7.hys	317.4267	452.8941	8.637616	2647953	345.4987	356.7513	4.702985	0.171036	0.001282	220.4645	2.599267
b-8.hys	161.6803	470.1429	3.790721	761164	261.5095	254.6988	3.849617	0.617663	3.029445	125.9128	1.03839
b-9.hys	265.0212	466.2634	12.02431	1881852	291.8244	294.1038	7.766089	0.247768	0.000363	179.1542	2.964396
							4.806204	**0.359419**			
t-1.hys	257.0515	471.2712	10.75493	1777029	287.04	289.9158	7.148176	0.265202	7.02E-05	150.4274	3.18328
t-10.hys	201.5287	461.2983	4.995671	1132175	272.0592	270.7848	4.159712	0.407444	0.989784	152.0169	1.286182
t-2.hys	186.1135	473.0233	7.791622	979577.2	231.0638	231.6455	6.974986	0.482885	0.005805	92.54182	2.29131
t-3.hys	277.1402	464.3624	13.90673	2047156	297.9	302.1836	8.611608	0.226833	0.000123	194.1672	3.234874
t-4.hys	244.6294	461.6928	6.342293	1619790	297.4269	299.2263	4.415214	0.285033	0.080015	169.6243	1.780347
t-5.hys	300.8863	449.3649	6.101572	2391739	353.9506	356.1219	3.495584	0.187882	0.570359	250.6776	1.431744
t-6.hys	148.5164	473.7212	9.269358	655379.8	190.0398	186.846	10.14467	0.722819	0.546217	107.7408	1.547861
t-7.hys	226.8343	461.6652	7.674474	1407570	273.4481	271.9513	5.731237	0.327987	2.001849	196.2968	1.257639
t-8.hys	192.915	477.2725	10.19566	1045492	230.909	228.0235	8.834661	0.456505	0.106246	140.0816	1.878646
t-9.hys	172.7576	479.41	9.984963	856626.9	207.4713	208.7675	9.558405	0.559649	0.019316	104.2634	2.176571
							6.907425	**0.392224**			

2) Table C-2: Results for dentin after treatment with EDTA

File	hc(nm)	Pmax(μN)	S(μN/nm)	A(nm^2)	hmax(nm)	heff(nm)	Er(GPa)	H(GPa)	A	hf(nm)	m
b-1.hys	441.4549	449.42	3.33144	4993638	533.5969	542.6319	1.320865	0.089999	1.34E-05	151.1488	2.901968
b-2.hys	258.3941	452.8782	3.683255	1794472	348.796	350.6111	2.436117	0.252374	0.001	67.07107	2.306029
b-3.hys	536.9874	395.8614	1.435334	7311883	724.8687	743.8355	0.470298	0.054139	0.001172	188.3116	2.014246
b-4.hys	573.4681	390.6127	1.420595	8314719	767.6331	779.6912	0.436497	0.046978	0.00103	221.2553	2.030941
b-5.hys	709.2247	356.6589	0.83252	12617877	1017.191	1030.531	0.207652	0.028266	0.012179	354.3755	1.578296
b-6.hys	558.8058	381.7655	0.984079	7903845	841.4772	849.7622	0.310131	0.048301	0.00425	171.1367	1.749297
b-7.hys	277.1436	460.2892	4.402057	2047203	350.6849	355.5653	2.725901	0.224838	0.000794	104.4593	2.401497
b-8.hys	386.8057	429.2845	2.959132	3867709	493.2012	495.609	1.333129	0.110992	0.002785	192.3544	2.090386
							1.155074	**0.106986**			
t-1.hys	256.9202	474.5844	4.994321	1775328	323.8513	328.1888	3.321023	0.267322	0.00134	103.8819	2.360509
t-2.hys	346.5078	442.377	5.691109	3130699	401.7297	404.8062	2.849778	0.141303	0.000192	192.2877	2.734017
t-3.hys	411.6843	472.4728	9.541109	4362222	444.1856	448.8241	4.047434	0.10831	1.99E-05	284.0657	3.327129
t-4.hys	365.2845	431.1622	2.849374	3464264	479.7537	478.7731	1.356372	0.12446	0.006739	184.2406	1.946444
t-5.hys	458.462	390.7721	0.907565	5373750	772.4645	781.3909	0.346876	0.072719	0.025257	138.9409	1.492085
t-6.hys	604.0718	370.2559	0.93717	9206147	893.9803	900.3809	0.273662	0.040218	0.004784	218.7518	1.725299
t-7.hys	462.9535	413.9414	1.658659	5476494	646.1356	650.1265	0.627973	0.075585	0.006775	199.9738	1.803757
t-8.hys	408.7194	422.0594	1.930152	4301705	565.8276	572.7192	0.824529	0.098114	0.002274	136.3145	1.995756
							1.705956	**0.116004**			

APPENDIX D CALCULATIONS FOR EDTA TREATMENT

1) Decrease in Young's modulus for bottom surface

= (4.806204 - 1.155074) / 4.806204 X 100%

≈ 76.0%

2) Decrease in hardness for bottom surface

= (0.359419 – 0.106986) / 0.359419 X 100%

≈ 70.2%

3) Decrease in Young's modulus for top surface

= (6.907425 – 1.705956) / 6.907425 X 100%

≈ 75.3%

4) Decrease in hardness for top surface

= (0.392224 – 0.116004) / 0.392224 X 100%

≈ 70.4%

APPENDIX E NANOINDENTATION RESULTS FOR NaOCl TREATMENT

1) Table E-1: Results for dentin before treatment with NaOCl for Sample 1

File	hc(nm)	Pmax(μN)	S(μN/nm)	A(nm^2)	hmax(nm)	heff(nm)	Er(GPa)	H(GPa)	A	hf(nm)	m
b-1.hys	635.5597	417.333	5.626961	10171098	683.4838	691.1847	1.563237	0.041031	5.03E-05	471.9709	2.956692
b-10.hys	324.7315	441.8815	4.386971	2765342	396.3914	400.2759	2.337358	0.159793	0.000368	145.731	2.527106
b-2.hys	343.3408	435.647	3.780077	3076130	422.9232	429.7769	1.90956	0.141622	0.248138	261.7529	1.457932
b-3.hys	285.7728	452.3726	4.629283	2169256	356.7896	359.0627	2.784795	0.208538	0.086337	194.9816	1.679097
b-4.hys	339.031	444.5128	6.655863	3002654	383.8428	389.1199	3.403193	0.14804	0.000178	201.2432	2.813151
b-5.hys	257.4406	458.3712	5.228633	1782075	322.1015	323.1897	3.470244	0.257212	0.006511	136.1406	2.133667
b-6.hys	310.6477	456.7275	5.961	2541337	366.2591	368.1122	3.313011	0.179719	0.009465	205.7694	2.118825
b-7.hys	307.0643	446.76	5.434848	2485881	365.6848	368.7165	3.054091	0.179719	0.892192	259.7826	1.325184
b-8.hys	296.4249	441.8083	4.217167	2324909	371.9094	374.9981	2.450488	0.190033	0.74788	238.927	1.298831
b-9.hys	322.915	440.9738	3.736384	2735908	406.5987	411.4311	2.001408	0.16118	1.751899	278.0848	1.129647
							2.628739	**0.166689**			
t-1.hys	270.1132	456.3899	5.58521	1950439	326.5699	331.3987	3.543302	0.233993	0.004848	151.2222	2.204965
t-10.hys	354.3771	442.6061	3.965885	3268406	433.5443	438.0796	1.9436	0.13542	0.050683	245.5453	1.725166
t-2.hys	403.1011	435.519	6.900353	4188205	447.6097	450.4377	2.987392	0.103987	0.001881	295.7837	2.450335
t-3.hys	180.5113	454.5363	3.389893	926958.8	277.0958	281.0756	3.11954	0.490352	0.053705	57.01327	1.671038
t-4.hys	348.0754	440.0111	4.787783	3157890	412.7345	417.0026	2.387101	0.139337	0.064615	257.1479	1.739387
t-5.hys	396.4101	432.3378	4.3226	4055041	467.1672	471.4236	1.901876	0.106617	0.01484	276.4373	1.949512
t-6.hys	304.9242	445.9802	4.496995	2453060	374.7582	379.3039	2.543918	0.181806	0.019877	189.844	1.910399
t-7.hys	270.5759	452.8504	3.999961	1956734	351.4918	355.4862	2.533522	0.231432	0.07118	166.3506	1.670607
t-8.hys	344.6009	445.0905	4.646952	3097783	412.3326	416.4367	2.339255	0.14368	0.006315	214.9216	2.103912
t-9.hys	322.5697	444.7698	5.201941	2730332	381.9988	386.6953	2.789283	0.1629	0.001692	185.5301	2.352788
							2.608879	**0.192952**			

2) Table E-2: Results for dentin after treatment with NaOCl for Sample 1

File	hc(nm)	Pmax(μN)	S(μN/nm)	A(nm^2)	hmax(nm)	heff(nm)	Er(GPa)	H(GPa)	A	hf(nm)	m
b-1.hys	1460.962	249.9304	0.632294	52765259	1728.294	1757.419	0.077122	0.004737	2.96E-06	718.7155	2.627795
b-10.hys	474.7217	420.2663	4.190127	5750356	548.8666	549.9461	1.548156	0.073085	0.247284	400.8715	1.486299
b-2.hys	1949.729	186.1588	0.563345	93710227	2180.313	2197.568	0.05156	0.001987	3.95E-05	1432.767	2.314408
b-3.hys	962.0284	327.946	1.11433	23032826	1171.105	1182.753	0.205719	0.014238	0.008261	681.4991	1.703212
b-4.hys	969.284	328.8725	1.08168	23377895	1187.992	1197.313	0.198212	0.014068	0.02204	723.0937	1.559733
b-5.hys	1225.358	292.3978	0.995393	37206637	1429.968	1445.672	0.144564	0.007859	2.95E-06	637.7688	2.750298
b-6.hys	1439.387	271.6937	1.292361	51227417	1583.634	1597.06	0.159981	0.005304	1.27E-06	970.9418	2.978245
b-7.hys	1018.037	342.0344	3.30064	25763357	1092.422	1095.757	0.576145	0.013276	1.347784	975.891	1.15671
b-8.hys	470.0182	420.8912	4.456895	5640088	541.002	540.8452	1.66274	0.074625	0.010264	349.8668	2.022305
b-9.hys	450.7093	426.3517	5.210949	5198726	506.5048	512.0731	2.024898	0.082011	0.003922	329.8045	2.227721
							0.664912	**0.029119**			
t-1.hys	374.6047	433.3949	3.797017	3636214	457.6848	460.2103	1.76422	0.119188	0.069772	270.2117	1.664597
t-2.hys	364.1729	436.3265	3.85655	3444038	442.3601	449.0272	1.841195	0.12669	0.067043	259.5846	1.674422
t-3.hys	646.538	393.9373	3.381326	10518921	729.4693	733.9159	0.923711	0.03745	0.318625	571.0442	1.397994
t-4.hys	508.8415	410.1741	2.642238	6582585	618.6198	625.2696	0.912449	0.062312	0.532434	429.6944	1.259846
t-5.hys	551.9747	408.07	3.507018	7716009	637.1299	639.2433	1.118604	0.052886	0.003692	393.7124	2.110131
t-6.hys	1229.063	313.1886	3.091628	37430275	1302.321	1305.04	0.447724	0.008367	0.064742	1137.263	1.656207
t-7.hys	286.6858	446.7372	4.182184	2182380	364.1578	366.8001	2.508261	0.204702	0.23062	207.3795	1.492435
t-8.hys	334.2307	440.3263	4.259686	2921878	411.3281	411.7586	2.20791	0.1507	0.116182	245.236	1.610928
							1.465509	**0.095287**			

3) Table E-3: Results for dentin before treatment with NaOCl for Sample 2

File	hc(nm)	Pmax(μN)	S(μN/nm)	A(nm^2)	hmax(nm)	heff(nm)	Er(GPa)	H(GPa)	A	hf(nm)	m
b-1.hys	297.9631	443.5409	3.468739	2347840	388.3669	393.8641	2.005729	0.188914	0.081751	187.5516	1.61348
b-10.hys	291.7826	447.3556	3.806524	2256396	374.4219	379.9252	2.245204	0.198261	0.007435	143.3259	2.01321
b-2.hys	241.6061	454.9491	3.758146	1582653	327.4298	332.3986	2.646767	0.28746	0.07098	132.1662	1.654038
b-3.hys	341.2418	443.1012	4.633989	3040232	407.5555	412.9567	2.354705	0.145746	0.004245	205.7829	2.166641
b-4.hys	297.0707	447.7312	4.640466	2334522	366.2781	369.4338	2.690899	0.191787	0.003721	158.5225	2.185969
b-5.hys	283.4797	449.0517	4.383079	2136468	355.6196	360.3181	2.656843	0.210184	0.138694	197.6803	1.587466
b-6.hys	326.4755	444.3753	5.076724	2793752	387.9886	392.1244	2.691067	0.15906	0.046128	233.623	1.810784
b-7.hys	251.8003	456.3974	4.710925	1709647	321.0804	324.4608	3.192183	0.266954	0.016627	135.5506	1.949928
b-8.hys	316.3403	447.2636	4.671702	2630716	384.0583	388.1444	2.551955	0.170016	0.001626	166.1876	2.318356
b-9.hys	434.633	428.4243	3.557678	4845131	520.1741	524.9498	1.432019	0.088424	0.003545	270.5331	2.112702
							2.446737	**0.190681**			
t-1.hys	273.0712	450.9224	4.990274	1990859	339.5412	340.8413	3.133567	0.226496	0.000988	122.264	2.418955
t-10.hys	495.1884	424.4458	5.753616	6242746	546.1865	550.5161	2.040271	0.06799	0.005119	386.6625	2.221134
t-2.hys	314.0297	444.5497	4.193061	2594247	386.6651	393.545	2.306537	0.17136	0.491973	248.5467	1.367646
t-3.hys	184.1773	463.2593	4.957879	961220.2	252.4716	254.2566	4.480426	0.481949	0.075652	93.8038	1.717192
t-4.hys	346.3114	445.8151	6.902485	3127301	389.0576	394.7521	3.458243	0.142556	0.00011	207.0224	2.90659
t-5.hys	270.349	453.2058	5.395006	1953645	330.9164	333.3525	3.419825	0.23198	0.000483	118.2606	2.560475
t-6.hys	692.5409	387.6445	3.235633	12040489	777.5568	782.3945	0.826175	0.032195	0.000254	483.1905	2.497428
t-7.hys	320.9375	443.5594	4.315715	2704048	393.3617	398.0208	2.325307	0.164035	3.628342	292.086	1.030718
t-8.hys	748.8395	382.7609	4.523435	14043380	810.3874	812.3025	1.069467	0.027256	0.058467	663.6492	1.756771
t-9.hys	312.1709	445.7518	4.957503	2565098	376.9492	379.6069	2.742495	0.173776	0.000972	161.8729	2.421565
							2.580231	**0.171959**			

4) Table E-4: Results for dentin after treatment with NaOCl for Sample 2

File	hc(nm)	Pmax(μN)	S(μN/nm)	A(nm^2)	hmax(nm)	heff(nm)	Er(GPa)	H(GPa)	A	hf(nm)	m
b-1.hys	479.3627	424.0257	6.506624	5860217	525.2741	528.2389	2.381407	0.072357	0.000202	346.0041	2.796372
b-2.hys	391.1841	434.6814	5.888977	3952552	446.6544	446.5437	2.624436	0.109975	0.265337	331.4309	1.559525
b-3.hys	335.4228	439.8675	4.077344	2941834	414.0074	416.3335	2.106217	0.149521	2.042095	295.4544	1.120486
b-4.hys	316.4877	442.6815	4.769035	2633051	383.2934	386.1058	2.603968	0.168125	0.085393	229.0849	1.691595
b-5.hys	711.4157	387.1149	3.815765	12694716	782.3015	787.5043	0.948866	0.030494	2.694905	679.8079	1.061556
b-6.hys	1384.024	293.3053	4.463655	47385649	1432.439	1433.307	0.574516	0.00619	0.00118	1272.599	2.445723
b-7.hys	382.6586	432.3919	3.809621	3788210	463.5361	467.7836	1.734202	0.114141	0.290112	304.9407	1.434739
b-8.hys	419.8394	428.3471	4.649989	4530888	489.9557	488.9278	1.935508	0.094539	0.005901	293.4822	2.121691
							1.86364	**0.093168**			
t-1.hys	361.9931	436.5948	4.118131	3404552	435.4572	441.5064	1.977448	0.128239	3.296417	331.3366	1.039163
t-2.hys	317.4473	446.3957	6.213684	2648281	370.9881	371.3279	3.383	0.168561	0.001709	197.5862	2.418428
t-3.hys	343.0536	439.268	4.220183	3071204	420.9992	421.1191	2.133594	0.143028	4.220183	317.0317	1
t-4.hys	276.8231	446.2958	3.572517	2042740	366.8941	370.5167	2.214637	0.218479	0.610787	208.5887	1.296204
t-5.hys	449.8582	424.0902	3.937612	5179691	524.2822	530.635	1.532907	0.081876	0.315722	376.6231	1.429977
t-6.hys	419.7854	433.1919	5.875668	4529761	471.9947	475.0802	2.445988	0.095632	3.10E-05	250.9448	3.040097
t-7.hys	325.2417	443.4644	5.613793	2773639	388.0399	384.4883	2.986526	0.159885	0.00802	216.188	2.130506
t-8.hys	339.7445	437.1741	4.01007	3014756	418.8872	421.5089	2.04626	0.145011	0.948836	285.4282	1.248228
							2.340045	**0.142589**			

5) Table E-5: Results for dentin before treatment with NaOCl for Sample 3

File	hc(nm)	Pmax(μN)	S(μN/nm)	A(nm^2)	hmax(nm)	heff(nm)	Er(GPa)	H(GPa)	A	hf(nm)	m
b-1.hys	263.0203	451.5649	4.497816	1855245	336.5836	338.3177	2.925741	0.243399	0.195048	183.9692	1.537389
b-10.hys	371.6314	435.913	4.222037	3580899	446.472	449.0667	1.976791	0.121733	0.031973	261.3084	1.818534
b-2.hys	215.6837	459.9398	4.70895	1282404	287.5112	288.9389	3.684227	0.358654	0.048189	115.3648	1.777084
b-3.hys	287.3334	448.6941	4.202717	2191715	365.9886	367.4055	2.515203	0.204723	0.121943	196.8361	1.597648
b-4.hys	306.4576	445.4395	4.65451	2476554	376.5295	378.2331	2.620504	0.179863	0.170295	227.9835	1.569995
b-5.hys	345.9201	441.2489	5.193165	3120536	408.1613	409.6455	2.604668	0.141402	0.016647	240.8988	1.986021
b-6.hys	270.0024	450.3366	4.419258	1948932	344.1063	346.4298	2.804696	0.231068	0.194447	190.1444	1.533665
b-7.hys	331.2834	442.4499	4.522153	2872841	402.8385	404.6638	2.363874	0.154011	0.116722	245.618	1.625561
b-8.hys	199.3805	458.8563	4.242752	1110222	278.6109	280.4935	3.567612	0.413301	0.211118	117.3694	1.508305
b-9.hys	307.1283	445.0724	4.298684	2486866	382.9058	384.781	2.41515	0.178969	0.066152	208.364	1.703904
							2.747847	**0.222712**			
t-1.hys	365.6345	441.7352	2.6989	3470645	483.9032	488.3887	1.283561	0.127278	0.009086	180.1739	1.883121
t-2.hys	434.1223	422.9969	1.904816	4834106	590.0925	600.6726	0.767591	0.087503	0.011697	210.1025	1.758794
t-3.hys	291.0649	451.392	8.420202	2245897	329.6631	331.2711	4.978087	0.200985	0.009167	210.458	2.253629
t-4.hys	249.3607	472.8206	11.86191	1678797	276.6843	279.256	8.111296	0.281642	0.000213	157.8791	3.045049
t-5.hys	268.4689	460.8376	10.73189	1928153	301.7637	300.6746	6.84763	0.239005	0.001816	187.6465	2.632176
t-6.hys	319.9923	450.3447	8.361012	2688887	357.7954	360.3891	4.517596	0.167484	0.000783	216.6101	2.669375
t-7.hys	312.2627	449.8041	9.092337	2566534	347.3372	349.3658	5.028481	0.175257	0.001684	221.8645	2.57731
t-8.hys	282.9045	453.986	9.173951	2128285	317.6311	320.0194	5.571554	0.213311	0.002074	194.1683	2.543142
t-9.hys	446.0627	423.2635	3.466398	5095231	532.887	537.6413	1.360603	0.083071	0.027553	319.1361	1.789491
							4.274044	**0.17506**			

6) Table E-6: Results for dentin after treatment with NaOCl for Sample 3

File	hc(nm)	Pmax(μN)	S(μN/nm)	A(nm^2)	hmax(nm)	heff(nm)	Er(GPa)	H(GPa)	A	hf(nm)	m
b-1.hys	1121.359	332.643	5.37173	31203346	1168.791	1167.803	0.852017	0.01066	2.43E-06	951.9357	3.485961
b-10.hys	469.2977	423.6955	5.959505	5623292	518.2338	522.6195	2.226639	0.075347	0.000129	321.5057	2.828773
b-2.hys	344.3641	437.7259	3.982968	3093709	426.0592	426.7887	2.006328	0.141489	3.982968	316.8893	1
b-3.hys	440.9381	427.1887	5.421099	4982308	500.0831	500.0389	2.151825	0.085741	0.024682	347.1457	1.940242
b-4.hys	493.3502	420.4042	6.575515	6197687	546.2485	541.3013	2.340183	0.067832	0.000383	368.6632	2.700222
b-5.hys	427.8955	424.6142	3.757124	4700690	522.5195	512.6573	1.535357	0.09033	3.757124	399.6415	1
b-6.hys	427.1766	425.1658	3.132238	4685409	517.5175	528.9806	1.282082	0.090743	0.688808	359.1318	1.251293
b-7.hys	446.8199	426.655	4.176978	5112023	508.0929	523.4282	1.636819	0.083461	0.000372	266.5833	2.514527
b-8.hys	499.5788	413.529	3.315388	6351034	597.3521	593.1264	1.165593	0.065112	0.311292	419.2315	1.394169
b-9.hys	495.9023	414.1169	2.878894	6260289	592.4463	603.7866	1.019444	0.06615	0.032429	356.9062	1.716285
							1.621629	**0.077687**			
t-1.hys	743.3306	392.268	22.34959	13840555	753.0387	756.4942	5.322646	0.028342	0.000324	696.462	3.420355
t-2.hys	662.6278	399.6981	9.944649	11039335	693.6676	692.772	2.651874	0.036207	9.944649	652.5797	1
t-3.hys	629.7423	404.9824	10.36815	9989174	657.1412	659.0375	2.906508	0.040542	3.22E-06	512.8946	3.741475
t-4.hys	611.6304	404.7704	7.01336	9433361	658.501	654.916	2.023148	0.042908	0.002031	512.8266	2.46195
t-5.hys	618.4989	403.9709	6.082631	9642252	662.836	668.3093	1.73555	0.041896	0.095733	551.7923	1.754408
t-6.hys	557.31	415.1923	9.45797	7862520	586.9577	590.234	2.98849	0.052807	0.002077	476.9517	2.580539
t-7.hys	519.6143	418.437	6.762547	6857153	564.7353	566.021	2.288091	0.061022	0.007941	429.242	2.210546
							2.845187	**0.043389**			

7) Table E-7: Results for dentin before treatment with NaOCl for Sample 4

File	hc(nm)	Pmax(μN)	S(μN/nm)	A(nm^2)	hmax(nm)	heff(nm)	Er(GPa)	H(GPa)	A	hf(nm)	m
b-1.hys	266.0483	451.3821	5.193592	1895585	328.7619	331.2318	3.342189	0.238123	0.128151	188.2139	1.64556
b-10.hys	304.0301	446.7409	4.728043	2439412	373.1307	374.8957	2.682092	0.183135	0.058834	209.6066	1.749322
b-2.hys	257.3277	453.3984	5.129298	1780611	322.158	323.6231	3.405714	0.254631	0.168259	182.5475	1.595989
b-3.hys	261.812	452.4728	4.86006	1839272	329.9313	331.6372	3.175071	0.246006	0.233005	189.4401	1.527354
b-4.hys	294.3423	447.6858	4.709362	2294043	363.8207	365.6395	2.754838	0.195151	0.18148	217.1526	1.561985
b-5.hys	277.1233	450.1715	4.926935	2046921	344.0565	345.6504	3.051133	0.219926	0.156489	199.6343	1.598084
b-6.hys	228.6434	458.3885	4.484497	1428444	303.2244	305.3056	3.324428	0.320901	0.08531	134.5125	1.670899
b-7.hys	281.978	449.1535	4.714851	2115136	351.7659	353.4257	2.872326	0.212352	0.230923	208.4578	1.521755
b-8.hys	280.1491	448.7216	4.370504	2089303	355.2644	357.1519	2.678956	0.214771	0.092232	187.3849	1.653514
b-9.hys	283.7607	447.6129	4.479609	2140473	356.5155	358.7025	2.712814	0.209119	0.094756	193.2278	1.656033
							2.999956	**0.229412**			
t-1.hys	381.4883	440.8731	5.952698	3765929	432.3577	437.0354	2.71777	0.117069	0.005833	273.7633	2.204511
t-10.hys	319.6508	448.7133	7.646631	2683420	361.1862	363.6617	4.13581	0.167217	0.011508	235.7871	2.179141
t-2.hys	556.9097	397.5702	1.794334	7851479	708.5632	723.087	0.567365	0.050636	0.00177	275.7573	2.01891
t-3.hys	296.3303	451.4823	6.852824	2323501	343.7328	345.7423	3.983207	0.194311	0.003528	191.898	2.335125
t-4.hys	252.0695	456.0597	6.188519	1713069	303.6835	307.3404	4.189229	0.266224	0.159867	185.3015	1.656011
t-5.hys	259.867	459.3619	15.19964	1813709	282.5866	282.5334	9.99964	0.253272	0.234859	225.814	1.876768
t-6.hys	290.0707	455.0141	8.485686	2231395	327.5917	330.2867	5.033077	0.203915	0.006694	206.472	2.309056
t-7.hys	292.0583	452.4728	8.47518	2260434	329.3662	332.0992	4.994452	0.200171	0.001062	192.0622	2.623008
t-8.hys	259.211	456.9852	5.478741	1805129	323.0734	321.769	3.612946	0.253159	0.031994	164.0843	1.890463
t-9.hys	417.1274	433.8503	6.828191	4474438	461.4045	464.781	2.860034	0.096962	9.37E-05	278.2685	2.935444
							4.209353	**0.180294**			

8) Table E-8: Results for dentin after treatment with NaOCl for Sample 4

File	hc(nm)	Pmax(μN)	S(μN/nm)	A(nm^2)	hmax(nm)	heff(nm)	Er(GPa)	H(GPa)	A	hf(nm)	m
b-1.hys	651.9435	389.0438	2.528381	10692346	770.5736	767.3465	0.685079	0.036385	1.344994	597.5183	1.103707
b-2.hys	640.4568	395.536	3.268852	10325525	722.4284	731.208	0.90131	0.038307	6.45E-05	404.5267	2.699811
b-3.hys	802.5423	365.7842	2.00358	16098361	930.0153	939.4663	0.442436	0.022722	0.003977	584.1776	1.94609
b-4.hys	661.0999	389.2796	3.35077	10989374	747.9275	748.2321	0.895557	0.035423	3.203616	631.1499	1.007798
b-5.hys	646.9058	392.5317	2.887656	10530678	741.2515	748.8566	0.78841	0.037275	4.03E-05	378.9397	2.721291
b-6.hys	749.7302	380.0758	3.698167	14076314	831.7951	826.8108	0.873327	0.027001	1.47E-06	485.462	3.32135
b-7.hys	502.778	418.4279	5.1866	6430536	560.4439	563.2841	1.81215	0.065069	0.005153	386.9613	2.1856
b-8.hys	817.6314	370.2402	3.433961	16701143	898.5871	898.4943	0.744487	0.022169	3.003958	788.143	1.023503
							0.892845	**0.035544**			
t-1.hys	438.4272	428.7787	5.360649	4927447	492.1909	498.4169	2.139643	0.087018	5.323241	418.3265	1.001301
t-10.hys	538.6201	414.503	6.864826	7355375	591.072	583.9056	2.242652	0.056354	6.864826	523.5249	1
t-2.hys	440.2315	431.592	10.68064	4966838	475.1208	470.5381	4.24612	0.086895	0.000159	346.4004	3.072046
t-3.hys	570.9997	409.5777	4.896011	8244813	628.7713	633.7412	1.51073	0.049677	0.266405	506.9739	1.515351
t-4.hys	562.5094	412.5728	6.822999	8006638	601.9231	607.8604	2.136412	0.051529	2.58E-06	394.8143	3.523288
t-5.hys	555.6568	412.5088	6.176674	7816973	605.5516	605.7455	1.957358	0.052771	0.114603	490.536	1.725082
t-6.hys	466.6765	425.5062	6.99681	5562401	513.9669	512.2872	2.628474	0.076497	0.001179	357.8681	2.539191
t-7.hys	678.2349	393.6066	5.131422	11556227	735.0553	735.7638	1.33741	0.03406	0.001164	549.0283	2.434458
t-8.hys	460.7186	430.5813	18.90014	5425248	479.17	477.8051	7.189355	0.079366	0.004286	414.5381	2.777071
t-9.hys	566.8652	411.8284	6.539325	8128389	606.6441	614.0981	2.032196	0.050665	0.000122	432.1749	2.888714
							2.742035	**0.062483**			

APPENDIX F STATISTICAL RESULTS FOR NaOCl TREATMENT

Using Minitab 13.2, all tests are done at 0.05 level of significance.

1) Table F-1: Paired sample *t*- test for Young's modulus of top surface

	N	Mean	St Dev	SE Mean
Before	4	3.41750	0.95014	0.47507
After	4	2.35000	0.62626	0.31313
Difference	4	1.06750	0.57046	0.28523

95% CI for mean difference: (0.15977, 1.97523)

T-Test of mean difference = 0 (vs not = 0): T-Value = 3.74 P-Value = 0.033

2) Table F-2: Paired sample *t*- test for hardness of top surface

	N	Mean	St Dev	SE Mean
Before	4	0.180000	0.009274	0.004637
After	4	0.085750	0.043798	0.021899
Difference	4	0.094250	0.045683	0.022841

95% CI for mean difference: (0.021558, 0.166942)

T-Test of mean difference = 0 (vs not = 0): T-Value = 4.13 P-Value = 0.026

3) Table F-3: Paired sample *t*- test for Young's modulus of bottom surface

	N	Mean	St Dev	SE Mean
Before	4	2.70750	0.23071	0.11535
After	4	1.25750	0.57343	0.28672
Difference	4	1.45000	0.71833	0.35917

95% CI for mean difference: (0.30697, 2.59303)

T-Test of mean difference = 0 (vs not = 0): T-Value = 4.04 P-Value = 0.027

4) Table F-4: Paired sample *t*- test for hardness of bottom surface

	N	Mean	St Dev	SE Mean
Before	4	0.202500	0.028954	0.014477
After	4	0.059000	0.031337	0.015668
Difference	4	0.143500	0.038957	0.019479

95% CI for mean difference: (0.081510, 0.205490)

T-Test of mean difference = 0 (vs not = 0): T-Value = 7.37 P-Value = 0.005

APPENDIX G CALCULATIONS FOR NaOCl TREATMENT

1) Decrease in Young's modulus for bottom surface for Sample 1

= (2.628739 - 0.664912) / 2.628739 X 100%

≈ 74.7%

2) Decrease in hardness for bottom surface for Sample 1

= (0.166689 - 0.029119) / 0.166689 X 100%

≈ 82.5%

3) Decrease in Young's modulus for top surface for Sample 1

= (2.608879 – 1.465509) / 2.608879 X 100%

≈ 43.8%

4) Decrease in hardness for top surface for Sample 1

= (0.192952 – 0.095287) / 0.192952 X 100%

≈ 50.6%

5) Decrease in Young's modulus for bottom surface for Sample 2

= (2.446737 – 1.86364) / 2.446737 X 100%

≈ 23.8%

6) Decrease in hardness for bottom surface for Sample 2

= (0.190681 - 0.093168) / 0.190681 X 100%

≈ 51.1%

7) Decrease in Young's modulus for top surface for Sample 2

= (2.580231 – 2.340045) / 2.580231 X 100%

≈ 9.31%

8) Decrease in hardness for top surface for Sample 2

= (0.171959 – 0.142589) / 0.171959 X 100%

≈ 17.1%

9) Decrease in Young's modulus for bottom surface for Sample 3

= (2.747847 – 1.621629) / 2.747847 X 100%

≈ 41.0%

10) Decrease in hardness for bottom surface for Sample 3

= (0.222712 - 0.077687) / 0.222712 X 100%

≈ 65.1%

11) Decrease in Young's modulus for top surface for Sample 3

= (2.580231 – 2.340045) / 2.580231 X 100%

≈ 33.4%

12) Decrease in hardness for top surface for Sample 3

= (0.17506 – 0.043389) / 0.17506 X 100%

≈ 75.2%

13) Decrease in Young's modulus for bottom surface for Sample 4

= (2.999956 – 0.892845) / 2.999956 X 100%

≈ 70.2%

14) Decrease in hardness for bottom surface for Sample 4

= (0.229412 - 0.035544) / 0.229412 X 100%

≈ 84.5%

15) Decrease in Young's modulus for top surface for Sample 4

= (4.209353 – 2.742035) / 4.209353 X 100%

≈ 34.9%

16) Decrease in hardness for top surface for Sample 4

= (0.180294 – 0.062483) / 0.180294 X 100%

≈ 65.3%